

High-Performance Analog Products

Analog Applications Journal

First Quarter, 2013



IMPORTANT NOTICE

Texas Instruments Incorporated and its subsidiaries (TI) reserve the right to make corrections, enhancements, improvements and other changes to its semiconductor products and services per JESD46, latest issue, and to discontinue any product or service per JESD48, latest issue. Buyers should obtain the latest relevant information before placing orders and should verify that such information is current and complete. All semiconductor products (also referred to herein as “components”) are sold subject to TI’s terms and conditions of sale supplied at the time of order acknowledgment.

TI warrants performance of its components to the specifications applicable at the time of sale, in accordance with the warranty in TI’s terms and conditions of sale of semiconductor products. Testing and other quality control techniques are used to the extent TI deems necessary to support this warranty. Except where mandated by applicable law, testing of all parameters of each component is not necessarily performed.

TI assumes no liability for applications assistance or the design of Buyers’ products. Buyers are responsible for their products and applications using TI components. To minimize the risks associated with Buyers’ products and applications, Buyers should provide adequate design and operating safeguards.

TI does not warrant or represent that any license, either express or implied, is granted under any patent right, copyright, mask work right, or other intellectual property right relating to any combination, machine, or process in which TI components or services are used. Information published by TI regarding third-party products or services does not constitute a license to use such products or services or a warranty or endorsement thereof. Use of such information may require a license from a third party under the patents or other intellectual property of the third party, or a license from TI under the patents or other intellectual property of TI.

Reproduction of significant portions of TI information in TI data books or data sheets is permissible only if reproduction is without alteration and is accompanied by all associated warranties, conditions, limitations, and notices. TI is not responsible or liable for such altered documentation. Information of third parties may be subject to additional restrictions.

Resale of TI components or services with statements different from or beyond the parameters stated by TI for that component or service voids all express and any implied warranties for the associated TI component or service and is an unfair and deceptive business practice. TI is not responsible or liable for any such statements.

Buyer acknowledges and agrees that it is solely responsible for compliance with all legal, regulatory and safety-related requirements concerning its products, and any use of TI components in its applications, notwithstanding any applications-related information or support that may be provided by TI. Buyer represents and agrees that it has all the necessary expertise to create and implement safeguards which anticipate dangerous consequences of failures, monitor failures and their consequences, lessen the likelihood of failures that might cause harm and take appropriate remedial actions. Buyer will fully indemnify TI and its representatives against any damages arising out of the use of any TI components in safety-critical applications.

In some cases, TI components may be promoted specifically to facilitate safety-related applications. With such components, TI’s goal is to help enable customers to design and create their own end-product solutions that meet applicable functional safety standards and requirements. Nonetheless, such components are subject to these terms.

No TI components are authorized for use in FDA Class III (or similar life-critical medical equipment) unless authorized officers of the parties have executed a special agreement specifically governing such use.

Only those TI components which TI has specifically designated as military grade or “enhanced plastic” are designed and intended for use in military/aerospace applications or environments. Buyer acknowledges and agrees that any military or aerospace use of TI components which have **not** been so designated is solely at the Buyer’s risk, and that Buyer is solely responsible for compliance with all legal and regulatory requirements in connection with such use.

TI has specifically designated certain components as meeting ISO/TS16949 requirements, mainly for automotive use. In any case of use of non-designated products, TI will not be responsible for any failure to meet ISO/TS16949.

Products

Audio	www.ti.com/audio
Amplifiers	amplifier.ti.com
Data Converters	dataconverter.ti.com
DLP® Products	www.dlp.com
DSP	dsp.ti.com
Clocks and Timers	www.ti.com/clocks
Interface	interface.ti.com
Logic	logic.ti.com
Power Management	power.ti.com
Microcontrollers	microcontroller.ti.com
RFID	www.ti-rfid.com
OMAP™ Applications	
Processors	www.ti.com/omap
Wireless Connectivity	www.ti.com/wirelessconnectivity

Applications

Automotive and Transportation	www.ti.com/automotive
Communications and Telecom	www.ti.com/communications
Computers and Peripherals	www.ti.com/computers
Consumer Electronics	www.ti.com/consumer-apps
Energy and Lighting	www.ti.com/energy
Industrial	www.ti.com/industrial
Medical	www.ti.com/medical
Security	www.ti.com/security
Space, Avionics and Defense	www.ti.com/space-avionics-defense
Video and Imaging	www.ti.com/video

TI E2E™ Community

e2e.ti.com

Mailing Address: Texas Instruments, Post Office Box 655303, Dallas, Texas 75265

SSZZ022F

Contents

Introduction	4
Data Converters	
Grounding in mixed-signal systems demystified, Part 1	5
Maintaining system performance with ADCs and DACs in a noisy digital environment is dependent upon using good circuit-design techniques like proper signal routing, decoupling, and grounding. This article is the first of a two-part series that looks closely at the grounding techniques used in mixed-signal systems. Part 1 explains typical terminologies and ground planes and introduces partitioning methods.	
Add a digitally controlled PGA with noise filter to an ADC	9
Some application designs with a highly dynamic signal range can be enhanced by adding an external programmable gain amplifier (PGA) in front of the ADC. This article describes how to implement an economical PGA by using a single resettable integrator that allows gain to be digitally controlled and calibrated. In addition, the PGA provides low-pass filtering and the zero-level voltage reference can be externally controlled.	
Power Management	
Design of a 60-A interleaved active-clamp forward converter	13
Forward converters are typically avoided for supply outputs greater than 30 A or about 250 W. This article presents an interleaved forward-converter design capable of up to 60 A or about 500 W. This design retains the benefits of synchronous rectification while avoiding the problems of load sharing parallel supplies. A complete schematic, bill of materials, and test results are available.	
Power MOSFET failures in mobile PMUs: Causes and design precautions	17
Automotive and mobile systems can expose power MOSFETs to harsh operating environments and intense transients that result in component electrical overstress (EOS). This article addresses special design considerations and failure analysis of high-frequency switchers and regulators employing external feedback components for mobile applications. The discussion includes common device-failure mechanisms, general precautions, PCB layout techniques, and component-selection tips.	
35-V, single-channel gate drivers for IGBT and MOSFET renewable-energy applications	22
Renewable-energy applications present designers with challenges that include high voltages and power levels, extensive safety and reliability requirements, and overall complexity to interconnect multiple systems. This article describes how a single-channel gate driver contributes to meeting these challenges.	
How to pick a linear regulator for noise-sensitive applications	25
A low-noise power solution is essential to preserving signal accuracy and integrity. This article addresses criteria and parameters to consider in designing a low-noise power solution, including important specifications for picking a linear regulator.	
Index of Articles	28
TI Worldwide Technical Support	34

To view past issues of the
***Analog Applications Journal*, visit the Web site:**
www.ti.com/aaj

Subscribe to the AAJ:
www.ti.com/subscribe-aaj

Introduction

The *Analog Applications Journal* is a digest of technical analog articles published quarterly by Texas Instruments. Written with design engineers, engineering managers, system designers and technicians in mind, these “how-to” articles offer a basic understanding of how TI analog products can be used to solve various design issues and requirements. Readers will find tutorial information as well as practical engineering designs and detailed mathematical solutions as they apply to the following product categories:

- Data Converters
- Power Management
- Interface (Data Transmission)
- Amplifiers: Audio
- Amplifiers: Op Amps
- Low-Power RF
- General Interest

Analog Applications Journal articles include many helpful hints and rules of thumb to guide readers who are new to engineering, or engineers who are just new to analog, as well as the advanced analog engineer. Where applicable, readers will also find software routines and program structures.

Grounding in mixed-signal systems demystified, Part 1

By Sanjay Pithadia, Analog Applications Engineer,
and Shridhar More, Senior Analog Applications Engineer

Introduction

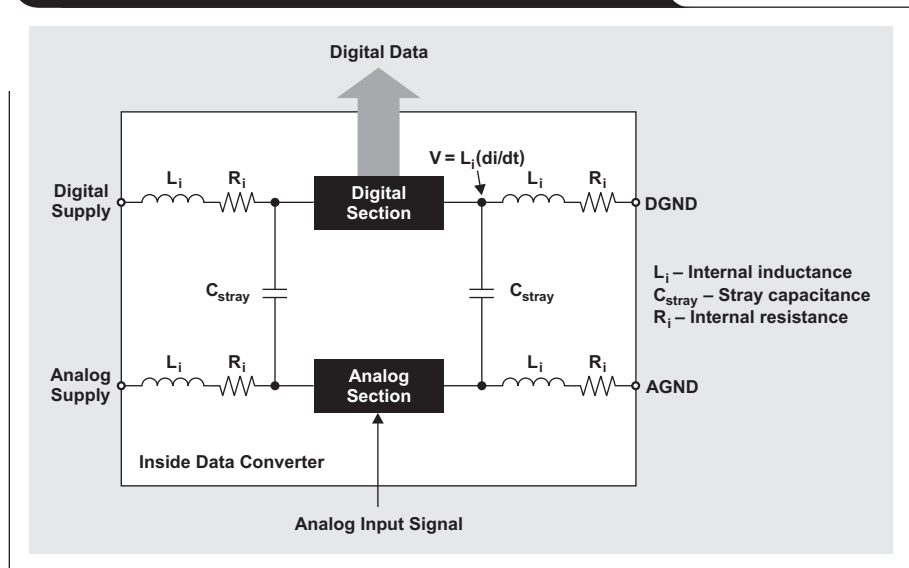
Every signal-processing system requires mixed-signal devices, such as analog-to-digital converters (ADCs) and/or digital-to-analog converters (DACs). The need for processing analog signals with a wide dynamic range imposes the requirement to use high-performance ADCs and DACs. Maintaining performance in a noisy digital environment is dependent upon using good circuit-design techniques like proper signal routing, decoupling, and grounding.

Undoubtedly, grounding is one of the most discussed subjects in system design. Though the basic concepts are relatively simple, the implementation is difficult. For linear systems, the ground is the reference against which the signal is based; and, unfortunately, it also becomes the return path for the power-supply current in unipolar supply systems. An improper application of grounding strategies can degrade the performance in high-accuracy linear systems. There is no “cookbook” that guarantees good results, but there are a few things that, if not done properly, can cause issues.

This article is the first of a two-part series that looks closely at the grounding techniques used in mixed-signal systems. Part 1 explains typical terminologies and ground planes and introduces partitioning methods. Part 2 explores techniques for splitting the ground planes, including pros and cons. It also explains grounding in systems with multiple converters and multiple boards. Part 2 will appear in a future issue of *Analog Applications Journal*.

A term often used in system design is *star ground*. This term builds on the theory that all voltages in a circuit are referred to as a single ground point, or star ground point. The key feature is that all voltages are measured with respect to a particular point in the ground network, not just to an undefined ground wherever one can clip a probe. Practically, it is difficult to implement. For example, in a star ground system, drawing out all signal paths to minimize signal interaction and the effects of high-impedance signal or ground paths causes implementation problems to arise. When power supplies are added to the circuit, either they add unwanted ground paths or their supply currents flowing in the existing ground paths are large enough or noisy enough to corrupt the signal transmission.

Figure 1. AGND and DGND pins in a data converter



Interpretation of AGND and DGND pins in mixed-signal devices

Digital- and analog-design engineers tend to view mixed-signal devices from different perspectives, but every engineer who uses a mixed-signal device is aware of analog ground (AGND) and digital ground (DGND). Many are confused about how to deal with these grounds; and, yes, much of the confusion comes from how the ADC ground pins are labeled. Note that the pin names, AGND and DGND, refer to what's going on inside the component and do not necessarily imply what one should do with the grounds externally. Data-converter datasheets usually suggest tying the analog and digital grounds together at the device. However, the designer may or may not want the data converter to become the system's star ground point. What should be done?

As illustrated in Figure 1, the grounds inside a mixed-signal IC are typically kept separate to avoid coupling digital signals into the analog circuits. An IC designer cannot do anything about the internal inductance and resistance (negligible compared to the inductance) associated with connecting the pads on the chip to the package pins. The rapidly changing digital currents produce a voltage (di/dt) in digital circuits, which inevitably couples into the analog circuits through the stray capacitance.

The IC works well in spite of such coupling. However, in order to prevent further coupling, the AGND and DGND

pins should be joined together externally to the same low-impedance ground plane with minimum lead lengths. Any extra external impedance in the DGND connection can cause more digital noise and, in turn, can couple more digital noise into the analog circuit through the stray capacitance.

Analog or digital ground plane, or both?

Why is a ground plane needed? If a bus wire is used as a ground instead of a plane, calculations must be done to determine the bus wire's voltage drop because of its impedance at the equivalent frequency of most logic transitions. This voltage drop creates an error in the final accuracy of the system. To implement a ground plane, one side of a double-sided PCB is made of continuous copper and is used as a ground. The large amount of metal has the lowest possible resistance and lowest possible inductance because of the large, flattened conductor pattern.

The ground plane acts as a low-impedance return path for decoupling high-frequency currents caused by fast digital logic. It also minimizes emissions from electromagnetic interference/radio-frequency interference (EMI/RFI). Because of the ground plane's shielding action, the circuit's susceptibility to external EMI/RFI is reduced. Ground planes also permit high-speed digital or analog signals to be transmitted via transmission-line (microstrip or stripline) techniques, where controlled impedances are required.

As mentioned earlier, the AGND and DGND pins must be joined together at the device. If the analog and digital grounds have to be separated, should both be tied to the analog ground plane, the digital ground plane, or both?

Remember that a data converter is *analog!* Thus, the AGND and DGND pins should be connected to the analog ground plane. If they are connected to the digital ground

plane, the analog input signal is going to have digital noise summed with it, because it is probably single-ended and referenced to the analog ground plane. Connecting the pins to a quiet analog ground plane can inject a small amount of digital noise into it and degrade the noise margin of the output logic. This is because the output logic is now referenced to the analog ground plane and all the other logic is referenced to the digital ground plane. However, these currents should be quite small and can be minimized by ensuring that the converter output does not drive a large fan-out.

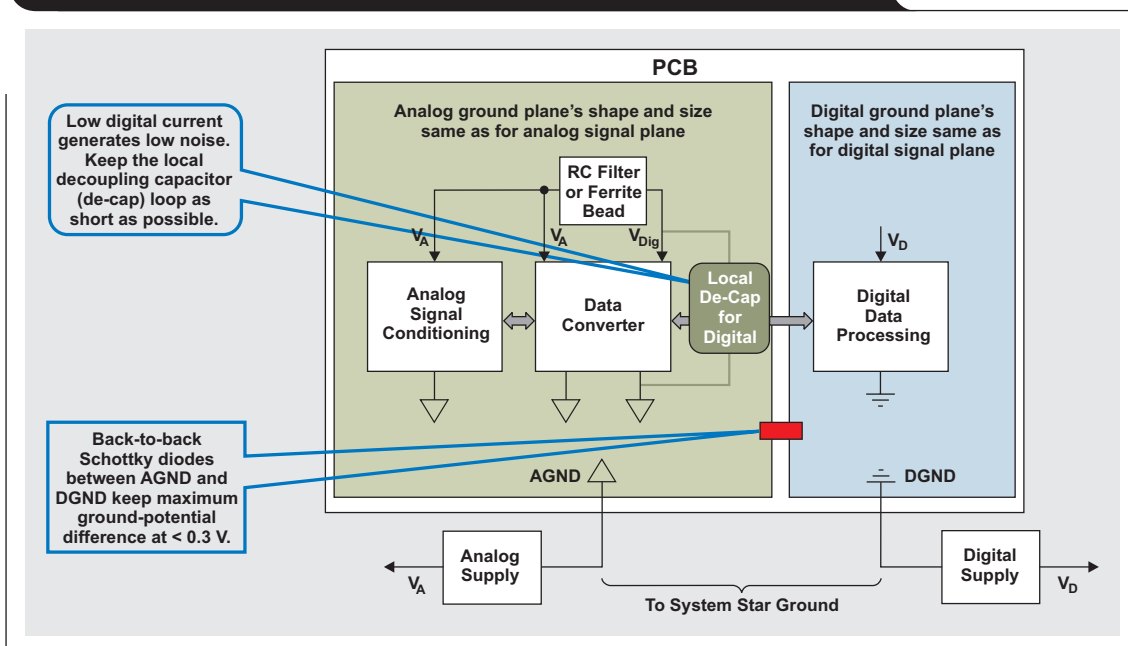
It is possible that the devices used in a design have either low digital currents or high digital currents. The grounding scheme is different for both cases. Traditionally, data converters may be thought of as low-current devices (such as flash ADC). But today's data converters with on-chip analog functions are becoming more and more digitally intensive. Along with the additional digital circuitry come larger digital currents and noise. For example, a sigma-delta ADC contains a complex digital filter that adds considerably to the digital current in the device.

Grounding data converters with low digital currents

As mentioned, a data converter (or any mixed-signal device) is analog. In any system, the analog signal plane is where all the analog circuitry and mixed-signal devices are placed. Similarly, the digital signal plane has all the digital data-processing circuits. The analog and digital ground planes should have the same size and shape as the respective signal planes.

Figure 2 summarizes the approach for grounding a mixed-signal device with low digital currents. The analog ground plane is not corrupted because the small digital

Figure 2. Grounding data converters with low internal digital currents



be made to work, it has many problems--especially in large, complex systems.

There are two basic principles of electromagnetic compatibility (EMC):

1. Currents should be returned to their sources locally and as compactly as possible. If not, a loop antenna should be created.
2. A system should have only one reference plane, as two references create a dipole antenna.

During EMC tests, most problems are observed when traces are routed across a slot or a split in a ground or power plane. Since this routing causes both radiation and crosstalk issues, it is not recommended.

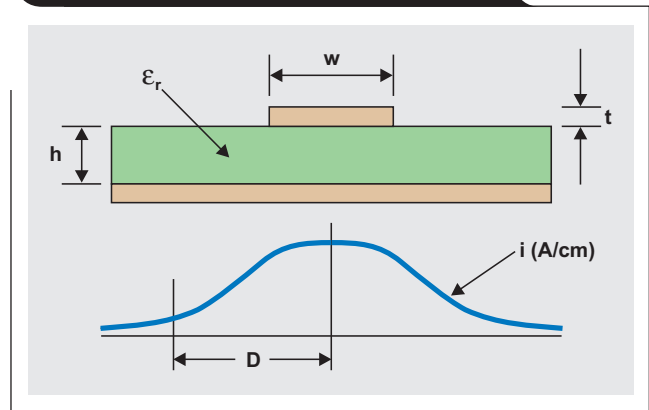
It is important to understand how and where the ground currents in a split plane actually flow. Most designers think only about where the signal current flows and ignore the path taken by the return current. The high-frequency signals have a characteristic of following the path of least impedance (inductance). The path's inductance is determined by the loop area that the path encloses. The larger the area that the current has to travel to return to the source, the larger the inductance will be. The smallest inductance path is directly next to the trace. So, regardless of the plane--power or ground--the return current flows on the plane adjacent to the trace. The current spreads out slightly in the plane but otherwise stays under the trace. The actual distribution is similar to a Gaussian curve in nature. Figure 4 illustrates that the return-current flow is directly below the signal trace. This creates the path of least impedance.

The current-distribution curve for the return path is defined by

$$i \text{ (A/cm)} = \frac{I_0}{\pi h} \times \frac{1}{1 + \left(\frac{D}{h}\right)^2},$$

where I_0 is the total signal current (A), h is the height of the trace (cm), and D is the distance from the trace (cm). From this equation it can be concluded that digital ground currents resist flowing through the analog portion of the ground plane and so will not corrupt the analog signal.

Figure 4. Distribution of return current



For reference planes, it is important that the clearance sections of vias do not interfere with the return current's path. In the case of an obstacle, the return current finds a way around it, as shown in Figure 5. However, this rerouting will most likely cause the current's electromagnetic fields to interfere with the fields of other signal traces, introducing crosstalk. Moreover, this obstacle adversely affects the impedance of the traces passing over it, leading to discontinuities and increased EMI.

Part 2 of this two-part article series will discuss the pros and cons involved in splitting the ground planes and will also explain grounding in systems with multiple converters and multiple boards.

References

1. H. W. Ott, "Partitioning and layout of a mixed-signal PCB," *Printed Circuit Design*, pp. 8–11, June 2001.
2. "Analog-to-digital converter grounding practices affect system performance," Application Report. Available: www.ti.com/sbaa052-aaJ

Related Web sites

Data Converters:

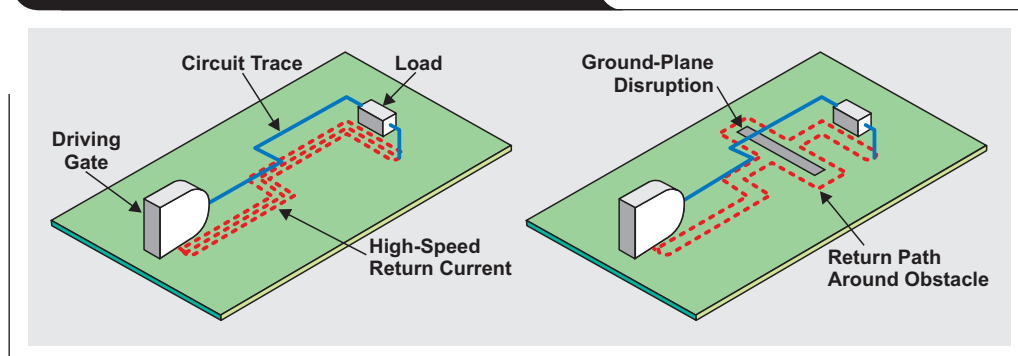
www.ti.com/dc-aaJ

For examples of grounding for precision data converters, visit: www.ti.com/e2egrounding-aaJ

Subscribe to the AAJ:

www.ti.com/subscribe-aaJ

Figure 5. Return current with and without slot



Add a digitally controlled PGA with noise filter to an ADC

By Kai Gossner

Field Application Engineer

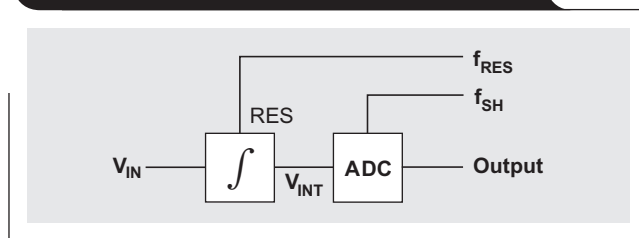
Introduction

In some applications, a signal with high dynamic range needs to be digitized. A common method of digitization is to add an external programmable gain amplifier (PGA) in front of the analog-to-digital converter (ADC). Only a few microcontrollers have internal PGAs. However, nowadays PGAs are available in a single chip with one or multiple input channels. Such PGAs add additional costs to the system and usually consume more power as a fixed-gain solution.

This article describes how to implement a PGA by using just a single resettable integrator, with the following benefits:

- The solution is economical and easy to design.
- Gain can be digitally controlled and calibrated.

Figure 1. Basic block diagram of the PGA



- Signal noise is reduced with a low-pass filter, which is especially useful in noisy microcontroller environments and for small analog signals. The cutoff frequency automatically adjusts with the chosen sample rate.
- The zero-level voltage reference can be controlled externally, which makes it handy for single-supply circuits where the zero level usually is set to $V_{REF}/2$.

The basic circuit

Figure 1 shows the basic circuit, where an integrator is added in front of the ADC. The integrator can be reset with the signal f_{RES} (1 = integrator is reset). The ADC is controlled with the signal f_{SH} , which connects to the ADC's sample-and-hold (SH) unit (1 = sample, 0 = hold). A falling edge starts the analog-to-digital conversion cycle.

Figure 2 shows a single analog-to-digital (A/D) conversion cycle with the circuit from Figure 1. The cycle is split into four periods:

1. *Integrator reset period:* Resets the integrator to "0."
2. *Integration period:* The integrator reset signal is released and the integrator starts to integrate.
3. *Sample period:* The ADC's sample-and-hold unit samples the integrator output, V_{INT} .
4. *A/D conversion period:* The sample-and-hold unit holds the voltage, and the ADC starts to convert.

Figure 2. Single A/D cycle with gain = 1

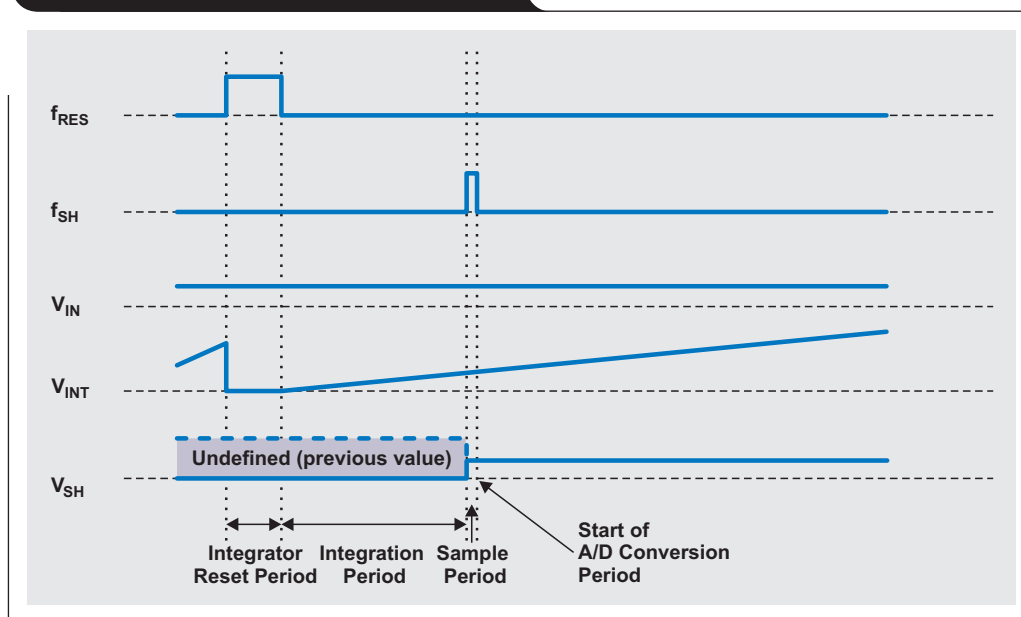
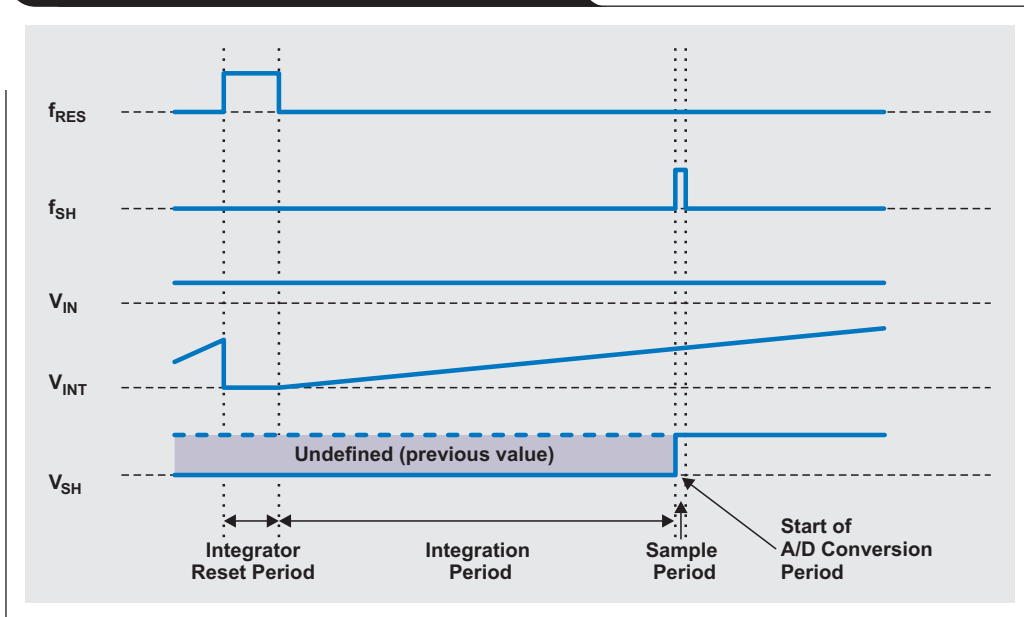


Figure 3. Single A/D cycle with PGA gain = 2



The duration of the integration period defines the PGA's gain, as the voltage on its input influences the slope linearly: A doubling of the integration time doubles the gain. Figure 3 demonstrates this influence. The integration period is doubled and the voltages V_{SH} are increased by a factor of two.

A nice benefit from this integration scheme is that the input signal is averaged during the integration period, which reduces out-of-band noise from the input signal, V_{IN} . The filter's impulse response is of finite duration and is comparable to the behavior of a digital FIR filter rather than to that of a standard low-pass filter.

Practical configuration of a PGA

An inverting amplifier can be built with a single operational amplifier (Figure 4). The integrator can be reset by short-circuiting the capacitor, C , with the switch element, S . The components R and C influence the integrator's gain.

The signal V_{COM} defines the integrator's zero-level voltage and can be set, for example, to $V_{REF}/2$, where V_{REF} is the ADC's reference voltage. The integrator is reset to this voltage when the capacitor is discharged. Usually a V_{COM} signal is present in the system anyway. Often it is used as a virtual ground or bias voltage for single-supply analog signal chains.

Figure 4. Practical configuration of the PGA

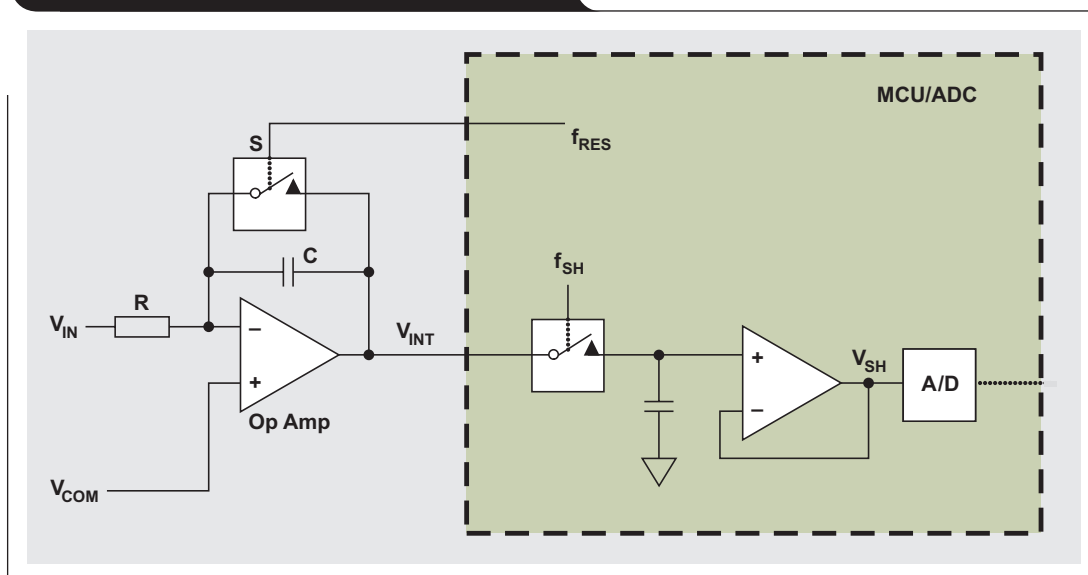


Figure 5. SPICE-simulation results of circuit in Figure 4

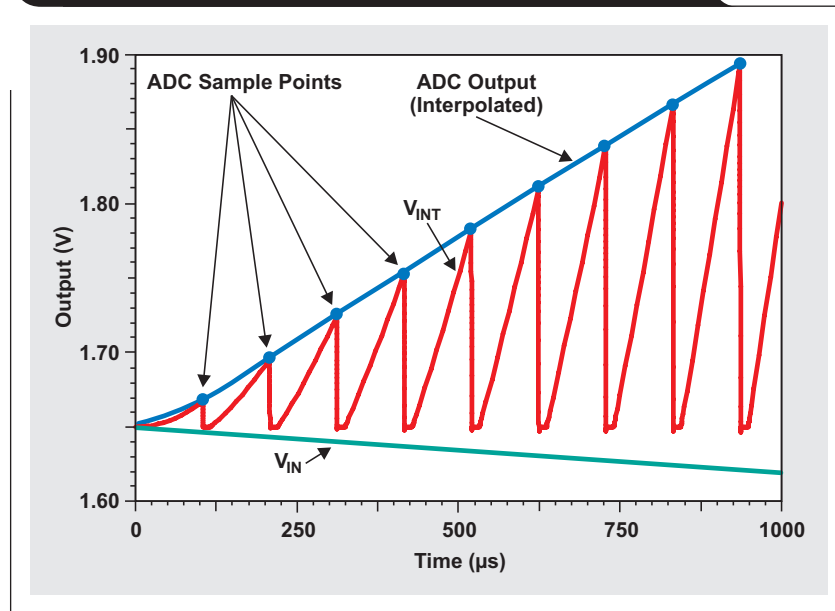


Figure 5 shows SPICE-simulation results of the circuit in Figure 4. The blue dots mark the sample moments of the ADC. As shown, the signal V_{IN} is amplified by a factor of about -8 . The red signal is inverted to the green due to the integrator's inverting behavior.

How it works

The sample rate, the maximum desired gain, and the A/D conversion time influence the selection of the integration constant defined by the components R and C. As shown in Figures 2 and 3, the integrator needs enough time to reach the gain, G, within the duration of the integration period, t. The dependency of G and t can be calculated as

$$G = \frac{-t}{R \times C}.$$

The close time (integrator reset period) of the switch (S) depends on the impedance of the switch and the value of the capacitor (C).

Calibration

Tolerances of R and C lead to modification of the gain factor. The capacitor should have a very small piezo effect to get a very linear integration. Capacitors can have an especially large tolerance--for example, 20%. This is just the initial tolerance, which can be calibrated once. Tolerances due to aging effects are very small (less than 1% per year).

The gain and offset can be calibrated in the same way as with a standard ADC by applying known voltages to the input and calculating correction values for offset and gain based on expected and actual values. The calibration can be done for each gain factor used in the application.

Circuit variations

Using the PGA as a low-pass filter only (gain = 1)

In case input-signal amplification is not wanted, it is possible to use the PGA circuit only as a noise filter. The integrator constant can be set to a value that leads to a fixed

gain of 1. In this case the integration phase can start immediately after the sample, and the hold stage can be set to hold mode (Figure 6).

Non-inverting integration

The circuit in Figure 4 uses an inverting integrator. When this inversion is not acceptable, it is possible to use a non-inverting integrator by adding a single-supply inverting buffer in front of the integrator.

Conclusion

This article has presented a cost-effective and simple way to implement PGA functionality in cost- and power-driven applications. Its filtering properties also reduce costs by eliminating the need for an external filter, which is often

present in front of ADCs. Nevertheless, this method cannot replace a PGA in all cases; for example, high sample rates or very large gain variations make such a solution difficult to realize.

Related Web sites

Data Converters:

www.ti.com/dc-aaj

www.ti.com/adc-aaj

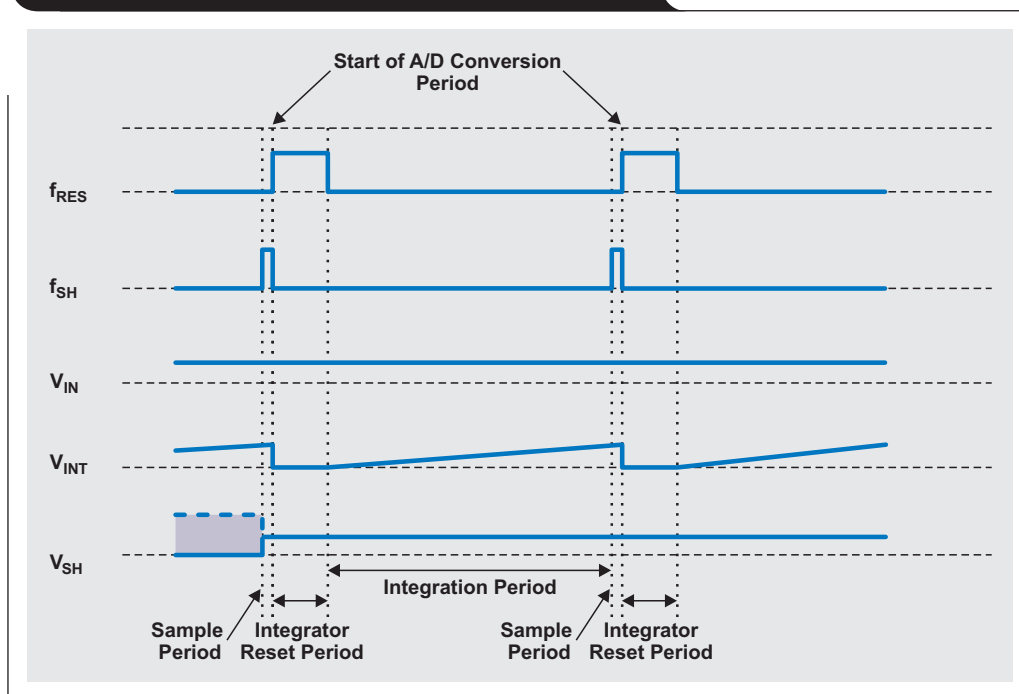
www.ti.com/e2edcforum-aaj

www.ti.com/msp430-aaj

Subscribe to the AAJ:

www.ti.com/subscribe-aaj

Figure 6. PGA circuit used as a filter only (gain = 1)



Design of a 60-A interleaved active-clamp forward converter

By Brian King

Applications Engineer, Member Group Technical Staff

Introduction

In 48-V-input telecommunications systems, power supplies with a capacity of 100 to 250 W are sufficient to cover many applications. Forward converters are a good choice for these applications. At lower output voltages, synchronous rectification in the secondary circuitry improves efficiency and simplifies system thermal design. Active-clamp forward converters work well in these applications because of the ease of implementing synchronous rectification.

In most cases, the output currents of forward converters are commonly limited to around 30 A. Beyond this current, the inductor design and conduction losses in the secondary circuitry become difficult to manage. From a power standpoint, the primary circuitry (number of parallel FETs) becomes a limiting factor for power ratings above 250 W. In systems with higher power, it is necessary to move to a different topology like the full bridge, or operate two or more forward converters in parallel to increase the output power.

Load-share ICs work great for paralleling supplies that use diodes to rectify their outputs. Diode-rectified supplies allow current to be sourced only from the power supply. Power supplies with synchronous rectifiers, however, can both source and sink power, which can wreak havoc with some load-share controllers. This is particularly true at start-up, where the feedback loop is overridden by the primary controller's slow-start circuit, and the two paralleled supplies could attempt to regulate the output to different voltage levels. These issues can be circumvented by interleaving two separate power stages. This article presents the design of a 5-V, 300-W interleaved isolated supply that is powered from a standard 36- to 72-V telecom input.

Designing the interleaved power stage

In this design example, splitting the power into two interleaved power stages reduces the current in the secondary of each phase to 30 A. This is much more manageable than the 60 A that would be required in a single-phase supply. Both phases actually need to be designed to carry a little more than 30 A to account for phase imbalances. Designing the power stage begins by selecting the turns ratio and inductance for the power transformers. A feature of the active-clamp forward converter is its ability to run at duty

cycles of over 50%. It is best to design for a maximum duty cycle of no greater than 75% so that the transformer's reset voltage does not become excessive. In this example, a turns ratio of 4.5:1 results in a duty cycle of around 63% at a 36-V input. Switching each phase at 200 kHz provides a good balance between size and efficiency. Setting the primary inductance at 100 μ H ensures that sufficient magnetizing current is flowing to drive the commutation of the power MOSFETs during the switching transitions. The primary inductance and switching frequency determine the value of the resonant capacitor in the clamp. In this case, a 0.1- μ F capacitor sets the resonant frequency at 50 kHz.

The output inductors are determined just as in any buck-derived topology. An inductance of 2 μ H is used, resulting in 8.5 A of peak-to-peak ripple current in each phase with a worst-case input of 72 V. Accounting for a 20% phase imbalance, the inductor must be able to carry at least 41 A of peak current without saturating.

The output capacitors are selected to meet the requirements for output ripple voltage and for voltage excursions due to load transients. Interleaving the power stages results in some cancellation of the ripple current seen by the output capacitors. The amount of ripple-current cancellation is dependent on the duty cycle and the phase angle between the two phases. Total cancellation occurs with a 50% duty cycle only when the two phases are synchronized 180° out of phase. This reduction in ripple current reduces the number of capacitors required based on the ripple-voltage requirements and the RMS current ratings of the capacitors. For this design, four 180- μ F polymer capacitors rated for 4-A RMS each are sufficient to keep the peak-to-peak ripple voltage below 50 mV. More capacitance can be added to support large load transients if necessary.

Selecting the primary MOSFETs is also straightforward. The peak drain voltage is the sum of the input voltage and the resonant transformer's reset voltage. The RMS primary current comprises the reflected load current and the transformer magnetizing current. It is important to select a minimal number of cost-effective transistors and to keep the power loss in each transistor manageable. For this design, each phase uses two 150-V, 50-m Ω MOSFETs in parallel, with a worst-case loss per FET of approximately 700 mW.

Figure 1 shows how self-driven synchronous rectifiers are implemented in each phase of the active-clamp forward converter. One set of synchronous rectifiers (Q4, Q5, and Q6) sees the input voltage reflected through the transformer, while the other set (Q1, Q2, and Q3) sees the transformer's reset voltage reflected to the secondary side. With the selected turns ratio, MOSFETs rated at 30 V are sufficient for this design. Most of the power loss in these components is due to conduction loss. Paralleling multiple 7-mΩ MOSFETs for each phase results in a worst-case loss

per FET of around 800 mW. This ensures that the junction temperatures are reasonable, even with a 20% phase imbalance. The gate-drive components Q12, Q13, Q15, and Q16 serve two functions. First, they protect the MOSFET gates from voltage spikes on the switching waveforms. Second, they provide a buffer so that the transformer's secondary windings are not directly connected to a large amount of gate capacitance. This is important to ensure that the power MOSFETs commute quickly during the switching transitions.

Figure 1. Gate-drive conditioning circuitry for a self-drive synchronous rectifier

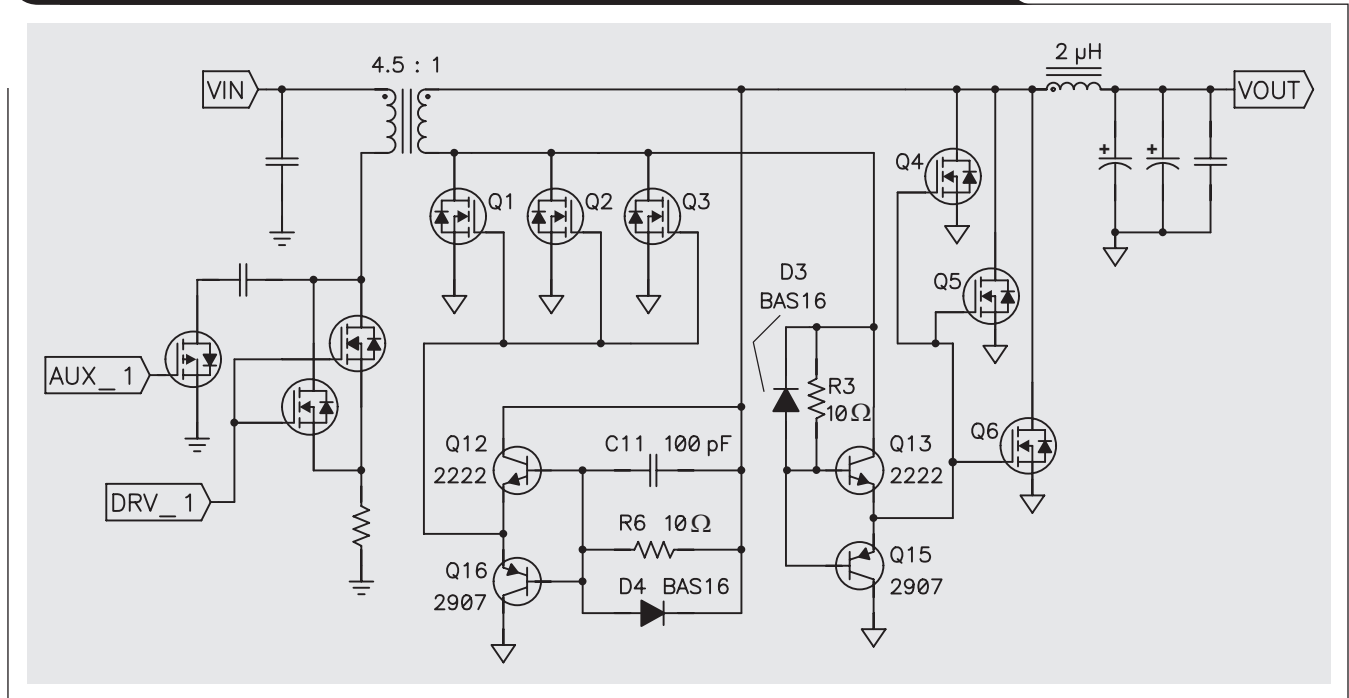


Figure 2. Interleaved controllers sharing feedback network and soft-start circuit

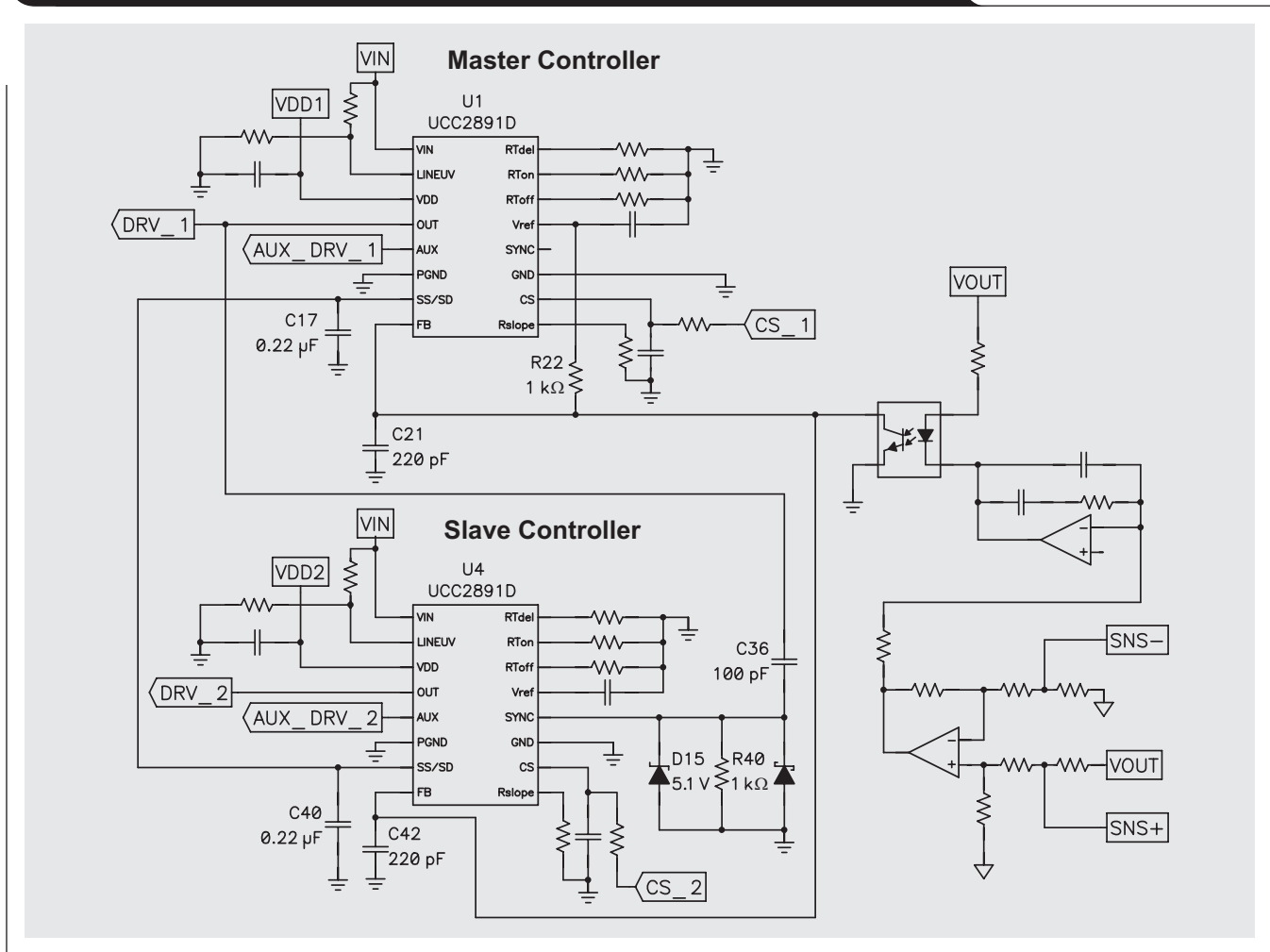
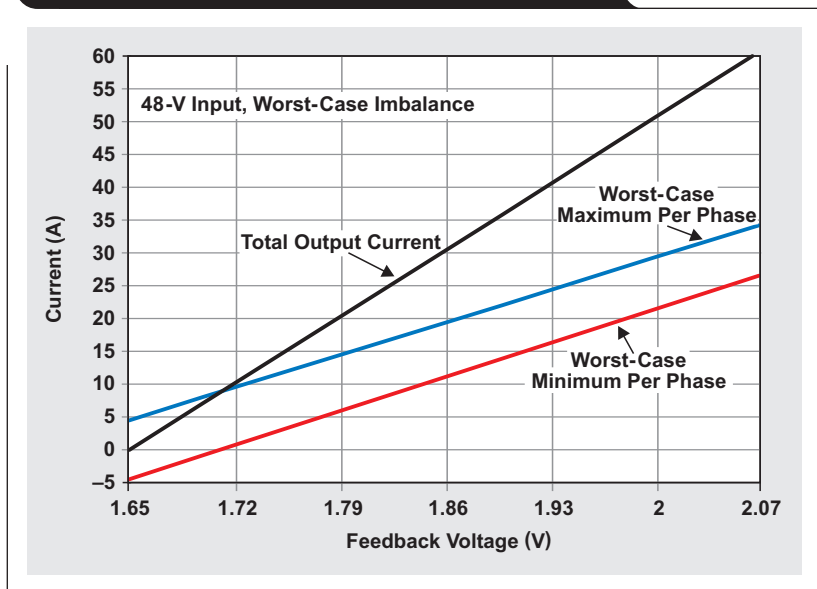


Figure 2 shows how two controllers can be connected in parallel so that they share a common feedback signal and soft-start circuit. With peak-current-mode control, each power stage behaves as a current source that is controlled by the voltage at the feedback pin. A single error amplifier regulates the output voltage by simultaneously controlling the feedback pins of the two controllers. Current imbalance between the two phases is mostly determined by variations of the offsets inside the controllers and by the tolerances of the current sense and slope compensation. Figure 3 plots the current in each phase versus the feedback voltage for a total tolerance resulting in the maximum error between phases. This is not of much concern at high load levels, as one stage will just carry a heavier burden. At light loads, however, the error can allow one phase to sink current, forcing the other phase to source extra current. This leads to increased losses at

Figure 3. Variation in offsets can lead to phase-current imbalance



light loads. The phase imbalance must also be considered when the current limit is programmed.

Synchronization is implemented by designating one controller as the master and the other as the slave. The clock frequency of the slave controller is set 10% slower than that of the master clock to ensure synchronization. The gate-drive signal of the master is used as the clock for the slave. Some conditioning components are needed to shape the magnitude and duration of the synchronization pulse.

For proper start-up, timing is critical. Start-up must be completed before the V_{DD} voltage on either chip falls below the UVLO OFF level, or neither controller will be able to start. Tying the two soft-start pins together ensures that both converters initiate the start-up sequence at the same time. In case of a fault, this also allows both controllers to be disabled by discharging the soft-start capacitance.

The efficiency of this power supply is shown in Figure 4. With a nominal 48-V input and a load current of 60 A, the supply's efficiency is over 92%. The converter's ability to convert to an isolated and regulated 5-V output with no intermediate bus and minimal power loss simplifies the system design and reduces the power demand on the upstream AC/DC rectifier.

Conclusion

In summary, interleaving active-clamp forward power stages can result in a cost-effective and efficient design. The design must account for current imbalances between the phases and ensure proper synchronization and start-up. If properly designed, interleaving extends the practical power range of the active-clamp forward converter to around 500 W and easily supports load currents of up to 60 A.

Please visit www.ti.com/tool/PMP2214 for more information on this design, including the complete schematic, bill of materials, and test results.

Related Web sites

Power Management:

www.ti.com/power-aaj

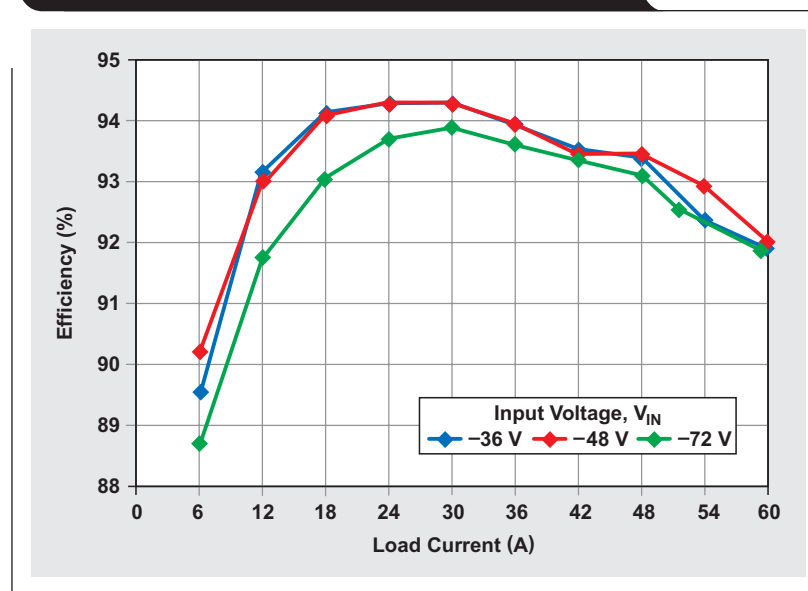
www.ti.com/ucc2891-aaj

www.ti.com/pmp2214-aaj

Subscribe to the AAJ:

www.ti.com/subscribe-aaj

Figure 4. Synchronous rectification enables very high efficiency



Power MOSFET failures in mobile PMUs: Causes and design precautions

By Kern Wong

Principal Applications Engineer

Introduction

Power MOSFETs in automotive systems and in mobile devices being charged or operated in automobiles may be subjected to harsh operating environments and intense transients from power equipment and transmitters.

Moreover, caustic contaminants in the atmosphere and on exposed conductive surfaces of circuit boards can induce low-impedance paths. Over time, these low-impedance paths and transient events like overloading, electromagnetic coupling, and inductively induced spikes from the operating environment can cause destructive electrical overstress (EOS) conditions. Such conditions may cause a large current to flow across a MOSFET power switch in a very short time.

This article addresses special design considerations and failure analysis of high-frequency switchers and regulators employing external feedback components for mobile and automotive applications. The goal is to help familiarize designers with various mechanisms and circumstances that may lead to destruction of on-chip power switches. Techniques for averting and eliminating the effects of EOS conditions are discussed to help improve end-user products and PCB designs. This article also presents tips for conducting lab tests and suggests good engineering practices to obviate potential problems from occurring in high-density/ultracompact mobile designs.^{1, 2}

Case studies

In 2011, a designer reported a shorted NMOS switch in the step-down DC/DC converter of the Texas Instruments (TI) LM26484 PMU during in-house testing. This regulator was designed into a new instrumentation panel. The banks of LEDs powered by a buck converter were operating in light-load conditions. TI asked the designers to monitor the voltage at the supply pins around the clock for transients above 6 V. They confirmed that transient spikes were peaking at over 8 V for hundreds of nanoseconds, which occurred frequently. The device's absolute maximum limit on the supply pin is $V_{IN} = 6\text{ V}$!

It was suspected that a parasitic NPN (formed by n+ (S), p- (well), and n+ (D) as shown in Figure 1) may have turned on hard when the p- (well) base biased up the emitter from n+ (S), a classic EOS scenario in power devices. Figure 2 shows an equivalent-circuit model of a MOSFET device with parasitic components.

Figure 1. Cross-section of a typical MOSFET structure and relevant parasitic elements

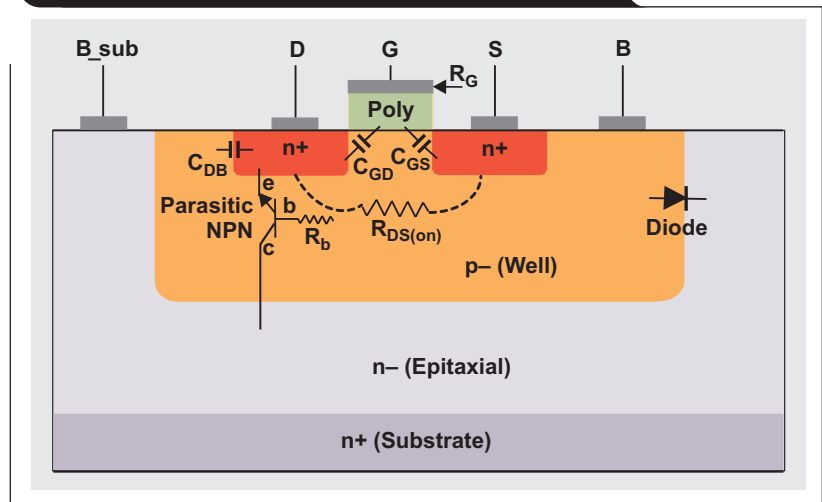
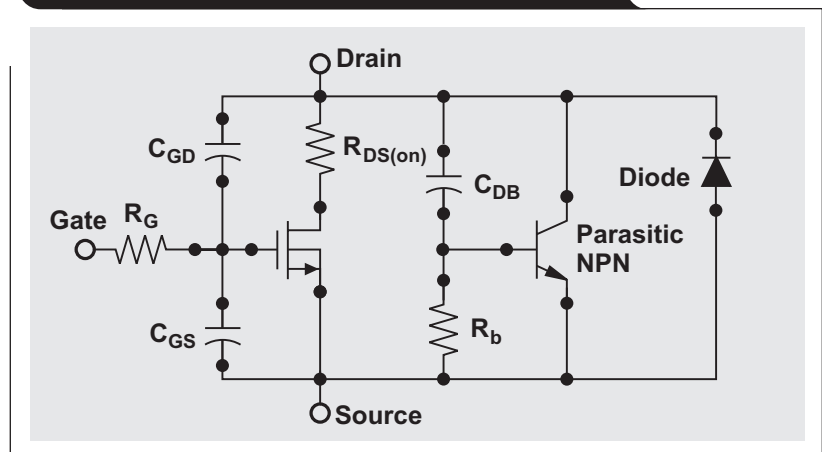


Figure 2. Model of a typical MOSFET with associated parasitic elements



Examining the PCB layout (Figure 3) revealed that the top traces of the power pins had a single via tapped into the power plane, and their longer tracks made the bypass capacitors ineffective. To prevent this situation from arising again, TI has suggested improved design guidelines. For example, adequately large bulk capacitors need to be added between the V_{IN} and ground planes. Also, local bypassing needs to be augmented with additional capacitors covering broader frequency bands. These precautions, shown implemented in Figure 4, will keep large transients from stressing the PMU's integrated circuit.

A more involved solution for eliminating EOS is to place the bypass capacitors closer to the power and ground pins, as shown in Figure 5. Note that the power-ground tracks have been widened and include liberal use of larger vias. This recommendation became a viable solution for the customer.

In 2012, another customer reported experiencing some failures with another PMU of the same family that had dual buck converters and dual LDOs. The buck-converter switches either shorted out or opened soon after the system left the factory. This PMU was powered from a stepped-down supply in an automotive application. With many infotainment and safety systems becoming standard equipment in cars starting in 2014, the PMU production rate is projected to increase by approximately tenfold, creating a concern for all parties involved. Although no anomalies have been discovered in the customer's rigorous testing for device- and board-level stress, some infrequent failures have occurred. In general, there are many known mechanisms and opportunities involved in vehicular applications that potentially could induce abnormal input-voltage transients, leading to device damage.

Common causes of EOS

Many EOS conditions on PMUs arise from inadequate design considerations or overlooking subtle parasitics in some systems. This is especially true in industrial/automotive applications, wherein unusual ambient conditions or differences in the electromechanical layout can manifest reliability issues. EOS can also be related to the manufacturing process, testing, and component aging.

The following discussion presents some of the most common EOS culprits. Appropriate design tips and suggestions are included to help designers eliminate EOS problems. A typical means of identifying failure mechanisms is well-documented. It is strongly suggested that readers seeking more information also study the physics of failure via failure-mode mechanisms and effects analysis (FMMEA).

Figure 3. PCB with two LM26484s provides four buck converters and two LDOs

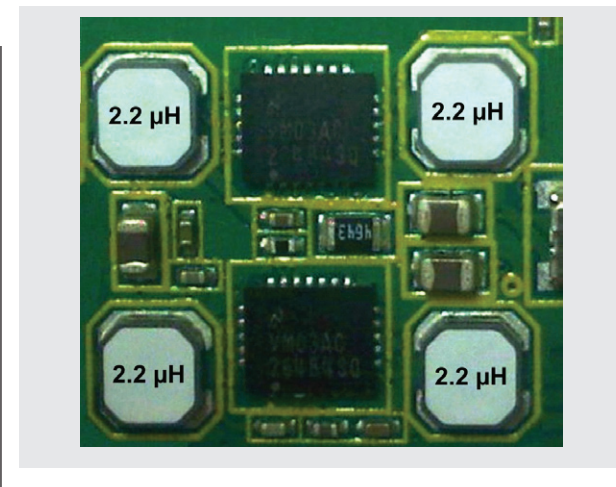


Figure 4. Example of a more robust line filter and bypass

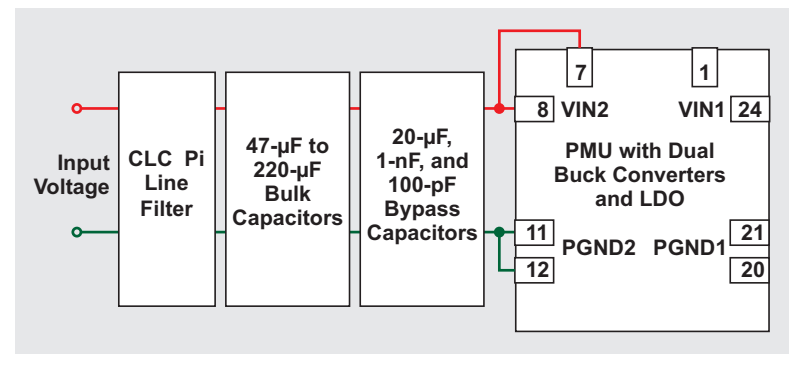
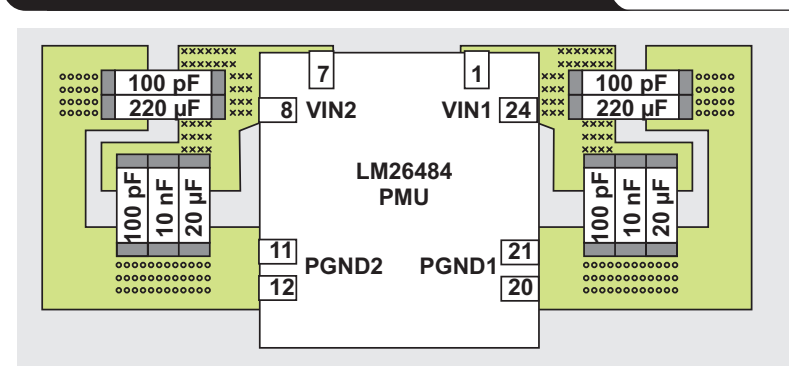


Figure 5. Improved layout with bypass capacitors closer to power and ground pins



EOS caused by battery and wiring in automotive applications

Whenever a vehicle's 12-V battery voltage falls too low, as in cold weather and cranking operations, the onboard PMU's control, timing, and decision-making circuits may malfunction before undervoltage lockout (UVLO) comes to its rescue. As a result, undesirable effects such as shoot-through and disengaged clamping can stress the MOS switches and cause permanent damage over time.

High-voltage, fast edge-rate transients are another commonly encountered cause of instantaneous device damage. Another example, load dumping, is when the 12-V battery is momentarily removed from the alternator connection. Due to the inductive effect from the long wirings involved, the loads can experience a sudden increase in potential at over 100 V, which may last for hundreds of milliseconds before it decays to normal levels.

High-voltage spikes in fast transients can propagate from the MOSFET's drain terminal to the gate via terminal capacitance. This can rapidly bias up the gate, potentially leading to runaway conditions. Normally, slightly exceeding the recommended maximum operating supply voltage might not be a destructive event. However, when the supply voltage exceeds the maximum level and sustains sufficient energy, it can cause the device to short-circuit in a few nanoseconds or lead to an avalanche breakdown. Moreover, loose or poorly secured battery-cable connections can manifest similar high-voltage transients if subjected to strong and abrupt mechanical vibrations.

Inadequate or poor power-supply bypassing

Inadequate supply bypassing can cause abnormal operation that may lead to shoot-through stress from timing issues. A proper bypass capacitor must have a voltage rating that adequately covers peak voltage transients. Leakage and parasitic inductance from traces are among the sources that cause the largest, most severe $L(di/dt)$ overstress pulses created at the pulsing terminal of a switcher. These high-energy pulses can lead to device breakdown as previously described. Hence, taking proper precautions to eliminate unwanted inductive paths is imperative. For example, bypass capacitors should be placed as close as possible to the device rail pins. A thick metal trace should be used as much as is allowable on all high-transient paths to further cut down parasitic inductance. Finally, transient-suppressing elements or similar techniques should be used as appropriate to attenuate potentially destructive high-voltage spikes.

Shorted output from overloading and/or a defective load capacitor

When a switcher's output current (I_{OUT} load) exceeds the rated limit, built-in protection circuits usually prevent any immediate damage to the device. However, frequent overcurrent events can lead to accumulated EOS conditions, which over time may cause permanent device damage. Such damage is associated with the finite delay time, typically in the range of microseconds, required before the protection circuit kicks into action. Other than true loading

shorts, a defective output capacitor can effect a low-impedance path that creates a dynamic short-circuit current in parallel with the maximum loading—thus producing another continuous EOS condition.

Temporary high-overcurrent operation with synchronous switches

The MOSFET body diode generally has a long reverse recovery time compared to that of the MOSFET switch itself. If the body diode of one MOSFET is still conducting when the opposing complementary device has switched on, then a short-circuit condition similar to shoot-through occurs. This can happen due to timing issues from parasitics or from the circuit or device design (see Figures 1 and 2). Furthermore, internal parasitic inductance and capacitance can store energy that, under certain conditions, additional current may freewheel through the body diodes of the FET switches as one turns off and the other turns on. This is the classic parasitic-capacitance mechanism, $C(dv/dt)$, with high-speed switching that can lead to continuous high-peak-current transients with no dependence on load conditions.

This type of EOS increases dramatically when coupled with power-rail integrity issues as discussed before. The circumstance can be improved or eliminated with more accurate design and simulation of the power-train circuitry and/or by augmenting protective devices, such as a Schottky diode across the drain and source of the MOSFET. Using a Schottky diode is a proven technique to prevent the body diode from being turned on by the freewheeling current. Eliminating excessive undershooting below ground that could cause noise and turning on parasitic pn junctions also lends another benefit—the Schottky diodes may moderately increase switcher efficiency.

Device-failure verification and analysis

Failure analysis (FA) utilizes visual inspection, impedance measurements, X-rays, SAT.Sam, emission hot-spot OBIRCH analysis, SEM, and SCM tools and techniques, etc., to identify failure-mode mechanisms and root causes of device failure. Failure analysis also examines whether general oversights in a customer's design or manufacturing process may be the cause. When the cause is identified, TI issues relevant advisory and containment actions to internal and external customers to help prevent failure from reoccurring.

Failure-mode mechanisms

1. Electrostatic-discharge (ESD) destruction or gate surge:

Device-junction or oxide-rupture damage (a short or leakage) can occur as a result of improper handling during assembly and testing of the device and system. These mechanisms introduce electrostatic charges onto the device and/or create external high-voltage surge events that reach the switch circuit.

For example, an ESD event between a fingertip and the communication-port connectors of a cell phone or tablet may cause permanent system damage. As process-technology nodes continue to shrink, device-level ESD

protection becomes inadequate on a system level. A transorb, or a transient-voltage suppressor such as TI's TPD1E10B06 protection diode, is a good remedy.

2. Wear-and-tear mechanisms:

- A die fracture may occur in extreme temperature cycling
- Over time, high-voltage stress may induce dielectric breakdown that will become a gate-oxide short circuit
- Wire bond and metal routes can open due to EOS from current overload, etc.
- A voltage transient on the supply lines can cause damage to passive and active devices on the die

3. PCB elements and environment:

- A circuit failure may occur due to humidity, presence of a contaminant, or filaments becoming conductive
- A die fracture may occur due to shock, vibration, material fatigue, etc.
- Loss of polymer strength, known as glass transition failure, may occur under high-temperature stress
- Bypass and load capacitors may be leaky or shorted
- Inductor windings may short-circuit due to wear and tear of insulation under high-temperature stress or mechanical vibration

4. Component aging and inadequacy:

Because aging components may contribute to MOSFET failures even if they initially meet datasheet specifications,¹ manufacturing and product-engineering departments are encouraged to perform testing and burn-in of parts at ratings slightly above datasheet limits. This ensures that marginal devices with inherent wafer-defect density and random process-related issues are weeded out. It may be better to lose some yield at production than to be accountable for and spend valuable resources on field failures later on.

Failure-analysis results

In the 2012 case study mentioned earlier, where the switch's drain and source channels were fused together in an automotive application, the customer could not determine that the PMU IC, the circuit board, or the subsystem had a reliability problem. Each was rigorously tested and stressed beyond specification limits, and no failure ever surfaced. The culprit might have been the layout; the electrical plumbing; the system installation; and/or the operating conditions, such as cold cranking, a weak battery, or intermittent connection of long/loose power cabling.

Because the customer and its subcontractors were unable to reproduce the initial failure in their lab, they needed confirmation and sought assistance from TI. Examples of in-house failure-analysis results are depicted in Figures 6 and 7.

Figure 6. High-side pFET shorted to the VIN rails

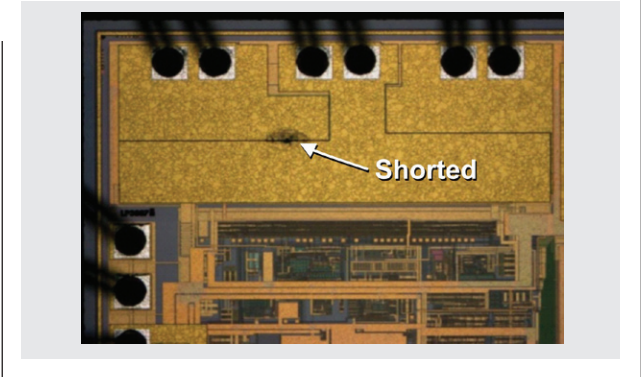
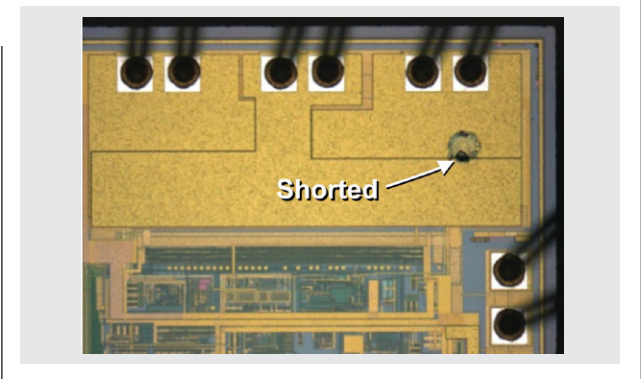


Figure 7. Low-side nFET shorted to ground



Failure analysis suggested that the burn marks reflected in the deprocessed dies were likely the consequence of EOS conditions. To validate this assumption, it was demonstrated that the failures could be induced in lab setups for (1) 5-V operation and (2) start-up conditions. By using a Keithley 2420 3-A source meter—a versatile power supply whose amplitude, frequency, and on/off times can be programmed— V_{IN} was programmed at 5 V and injected with a 50-ms pulse that repeated at 100-ms intervals. With loading at 200 mA and above, the pulse amplitude was increased at 0.5-V increments at 5-minute intervals until abnormal current was observed. The part was then decapped to visually confirm EOS. The results revealed that when the peak-to-peak pulse voltage reached approximately 7.5 V or more, the switches shorted out. Moreover, if pulses were to peak further to 9 V, the ESD structure might also be damaged.

Reproducing a short circuit from the switches during start-up was more challenging, however. With a bench supply cycling the buck converters on and off, V_{IN} issued relatively slow and smooth start-up transients and settled in at about 6 ms (Figure 8). Even with the supply set to slightly over 7 V, the switchers did not fail over days of stress testing.

In order to make the operation mimic in-vehicular conditions more closely, the cable length between the supply and the device was increased from about 30 cm to about 1.5 m. These longer wires, typically routed from the 12-V battery to the device, created more inductance. Furthermore, the soft power cycling from the power supply was replaced with a mechanical toggle switch such that the mechanical bounce and chatter behaved more like transients introduced by mechanical relay contacts (Figure 9).

The tests were conducted with the power-supply output set at 5.0 V, then the toggle switch was flip-flopped 20 times. If no overcurrent failure was detected, the supply voltage was increased by 0.2 V, the switch was again toggled on and off 20 times, and the process repeated until the part failed. The result was a stunning success! The buck converter's high- or low-side switch became shorted with the power-supply output at about 7.5 VDC. The V_{IN} pins monitored with a 10-pF probe exhibited faster turn-on transients, which caused an overshoot above 11 V in 20 μ s. The actual $L(di/dt)$ could have been a lot higher, creating a repeatable destructive EOS condition. The customer was elated that this bench setup replicated the same failures as in the field.

Conclusion

This article has discussed common device-failure mechanisms related to MOSFET transistors in integrated power-management and voltage-regulator circuits. General precautions, specific PCB layout techniques, and component-selection tips have been presented to help mitigate and eliminate EOS concerns. It is hoped that this article will help system and PCB designers be aware of the EOS effects of seemingly benign parasitic elements that can be subjected to transients in the PMU operating environment. Product and field support personnel may also find this article useful for understanding the cause and effect of EOS to facilitate their interface with customers.

Acknowledgments

The author thanks Ann Cocannon, Steven Jacobson, ChiYoung Kim, Maxwell Goodman, Andy Strachan, and Gavin Kirihara for their valuable input and support.

References

- 1 Kern Wong. (2012, April 27). "PCB and ESR subtleties in switching regulator and LDO designs." EDN [Online]. Available: www.edn.com

Figure 8. Power supply off/on ramping in ~6 ms

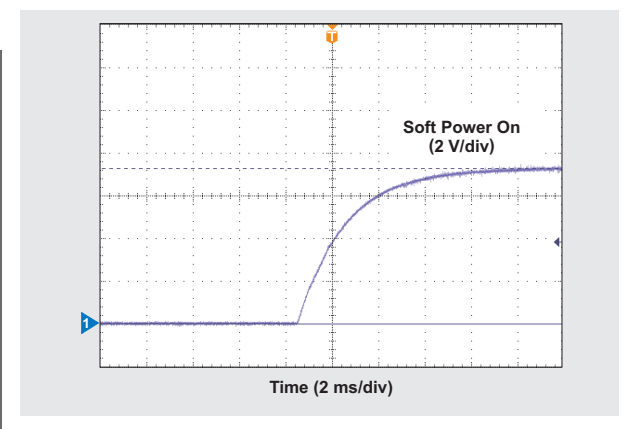
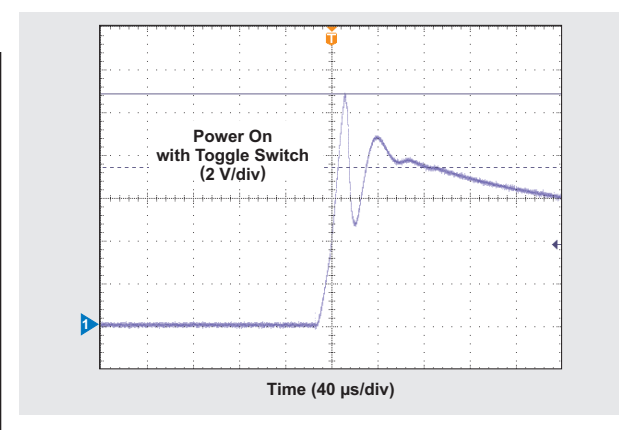


Figure 9. An 80- μ s transient induced by switch and longer wire



- 2 Kern Wong. (2012, June 21). "High-performance load- and line-transient test jigs for mobile regulators." EDN [Online]. Available: www.edn.com
- 3 "Power MOS FET application note," Rev.2.00, Renesas Electronics, REJ05G0001, Aug. 23, 2004 [Online]. Available: www.renesas.com (use Search, Advanced Search, Document Search to find REJ05G0001)
- 4 "Analysis of MOSFET failure modes in LLC resonant converter," Fairchild Semiconductor, AN-9067, Nov. 5, 2009 [Online]. Available: www.fairchildsemi.com/an/AN/AN-9067.pdf

Related Web sites

Power Management:

www.ti.com/power-aaaj

www.ti.com/lm26484-aaaj

www.ti.com/tpd1e10B06-aaaj

Subscribe to the AAJ:

www.ti.com/subscribe-aaaj

35-V, single-channel gate drivers for IGBT and MOSFET renewable-energy applications

By John Stevens

Systems Engineer, High-Performance Isolated Power

Introduction

The electronics market segment labeled as renewable energy is a complex and diverse arena for electric power conversion. In point-of-load applications, the switching power converter typically is non-isolated; power levels are fairly low (<200 W); and the power is usually converted from one DC voltage to another, such as from 12 V to 3.3 V. Further, the power-stage switches are integrated or capable of being driven by low-current controllers or transistors. Integration between the controller and power stage is being realized today. Silicon (Si) MOSFETs dominate this arena, where higher switching frequencies are preferred and can reach speeds of greater than 1 MHz. These power switches generally are driven by a 5- or 12-V IC gate driver or similar solution.

Challenges to efficiently managing renewable-energy systems

In the electronic power train from a wind or photovoltaic power generator, there are some unique performance challenges. Typical power levels for renewable energy can range from 1 to 3 kW for micro-inverters, 3 to 10 kW for string inverters, and 10 kW to 1 MW for large central-inverter stations. In addition to DC-to-DC conversion, DC-to-AC and AC-to-DC conversion can also be used, and sometimes a combination of the two.

Older wind turbines were tied directly to the power grid but had to run at the power-line frequency. This made them inefficient across the many operating points they experienced. Newer wind turbines (Figure 1) often convert AC to DC and then DC back to AC so that the wind-driven generator can run at variable speeds for maximum efficiency.

Conversely, photovoltaic cells produce DC voltage/current. Generally, the voltage is boosted higher and then sent through a DC-to-AC inverter before being tied to the grid.

Renewable-energy trends

For most countries, generating renewable energy from sources such as wind and solar power makes up only a small percentage of their total power portfolio. In recent history, growth has been consistent year by year. There are places where renewable energy makes up a large share of the available power. Denmark, for example, generated nearly 34% of its total electricity from wind power alone

in the first half of 2012, according to the Danish Energy Agency. According to its parent agency, the Danish Ministry of Climate, Energy and Building, Denmark has committed to having 50% of its total power supply come from wind by 2020. When wind energy makes up that large a portion of a country's total power, reliability of the conversion system becomes critical. This—together with the high-power connection to the grid, isolation safety requirements, and the cost of large renewable-energy conversion systems—means that system reliability is always the design priority, followed by efficiency. Therefore, protection features and reliability are preferred at all levels, from the controller all the way down to the FET/IGBT driver itself.

Typical power-management configuration

High power levels lead to higher system voltages, and therefore higher standoff voltages, for the components used within the converter. For lower power loss at greater than 400 V, most circuit designers prefer to use insulated-gate bipolar transistors (IGBTs) or the latest silicon carbide (SiC) FETs. These devices can have standoff voltages of up to 1200 V, with lower ON resistance than equivalent Si MOSFETs. These complex power systems often are managed by a digital signal processor, a microcontroller, or a dedicated digital power controller. Thus, they usually require both power and signal isolation from the noisy switching environment of the power stage. Even during steady-state switching cycles, the circuit can see massive changes in both voltage and current that can create significant ground bouncing.

Figure 1. Simplified power flow from wind turbine to grid

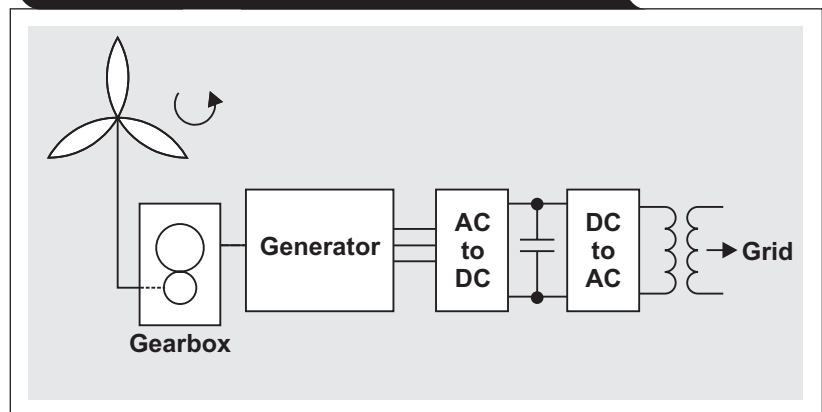


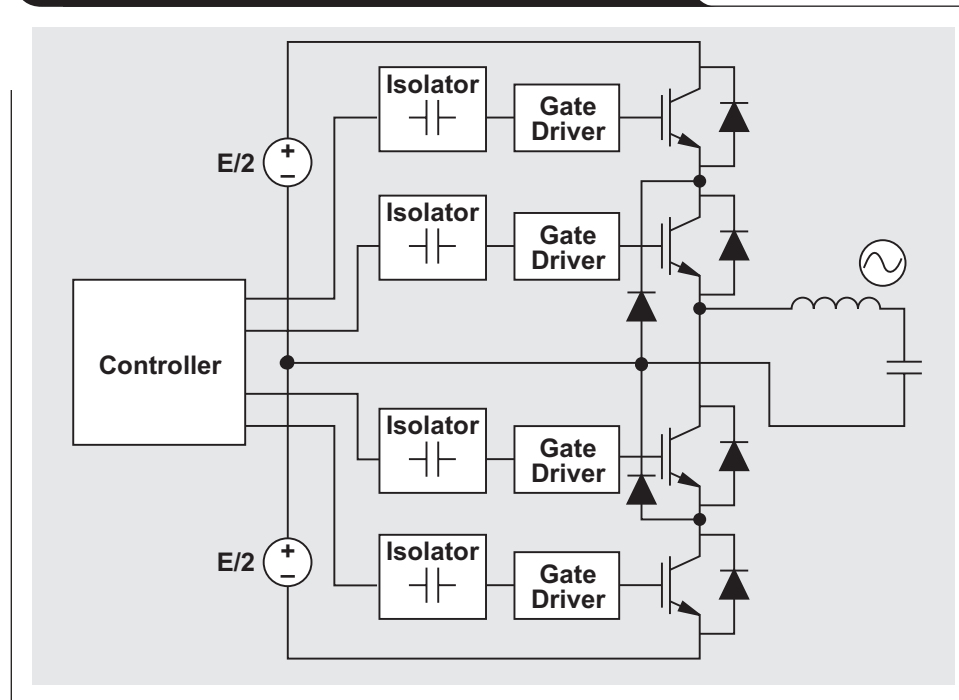
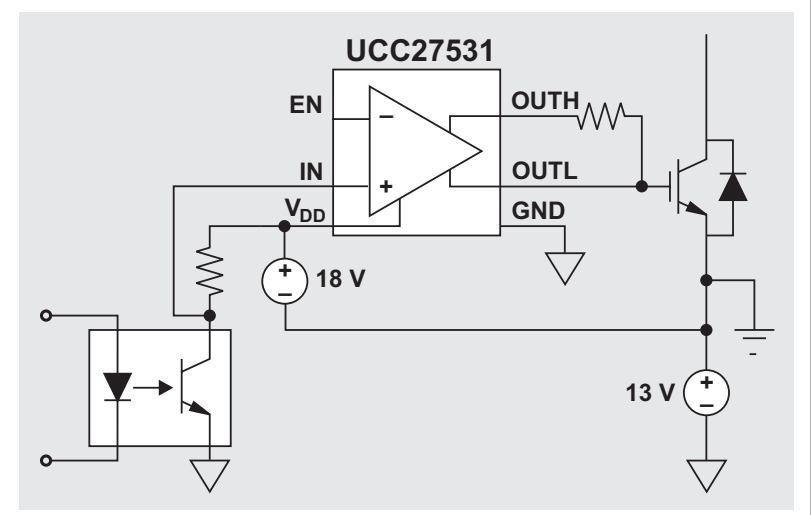
Figure 2. Basic structure of single-phase inverter

Figure 2 shows that even for a single-phase DC-to-AC inverter, there are many gate drivers needed to properly switch the IGBTs in the power stage. As a single-channel gate driver, the Texas Instruments UCC27531 can drive any of the switches in the switch bridge if it has the necessary signal and bias isolation. Signal isolation is achieved by using an optocoupler or digital isolator. For bias isolation, the designer can use a bootstrap circuit with a diode and a capacitor, or an isolated-bias supply. Another option is to connect the gate driver on the same side of the isolation as the controller, then drive the switch through a gate transformer after the gate driver itself. This option allows the driver to be biased with a non-isolated supply on the control side.

Gate drivers in renewable energy

As a small, non-isolated gate driver, the single-channel UCC27531 is a good fit for the environment described. Its input signals to the IC are provided by an optocoupler or digital isolator. Its high supply/output-drive voltage range of 10 to 35 V makes it ideal for 12-V Si MOSFET applications as well as for IGBT/SiC FET applications. Here, a higher positive gate drive is typical, as well as a negative voltage pull-down on shutoff to prevent the power switch from false turn-on. Typically, SiC FETs are driven by a +20/-5-V gate driver relative to the source. Similarly, for IGBTs, system designers may use a +18/-13-V gate drive, for example (see Figure 3).

Figure 3. Driving a power switch with FET/IGBT single-gate drivers

Since the UCC27531 is a rail-to-rail driver, OUTH pulls up the power-switch gate to its V_{DD} of 18 V relative to the emitter. OUTL pulls down the gate to the driver's GND of -13 V relative to the emitter. The driver effectively sees +18 to -13 V, or 31 V from V_{DD} relative to its own GND. Further, the 35-V rating provides a margin to prevent overvoltage failure of the IC due to noise and ringing.

The split output with both OUTH and OUTL permits the user to control the turn-on (sourcing) current and turn-off (sinking) current separately. This helps to maximize efficiency and maintain control of the switching times to

comply with requirements for noise and electromagnetic interference. Further, even with a split output, the single-gate driver maintains a minimum inductance on the output stage, preventing excessive ringing and overshoot. By having an asymmetrical drive (2.5-A turn-on and 5-A turn-off), the UCC27531 is optimized for average switch timing in high-power renewable-energy applications. Further, with the low pull-down impedance, this driver increases reliability by ensuring that the gate does not experience voltage spikes that could lead to false turn-on from the parasitic Miller-effect capacitance between the collector and gate for IGBTs and between the drain and gate for FETs. This internal capacitance can lead the gate to exceed the turn-on threshold voltage by pulling up on the gate when the collector/drain voltage rapidly increases during turn-off of the switch.

The input stage of the UCC27531 is also designed for high-reliability systems like renewable energy. It has a so-called TTL/CMOS input that is independent of the supply voltage, allowing for compatibility with standard TTL-level signals. It provides a higher hysteresis of about 1 V when compared to the usual 0.5-V hysteresis seen in classic TTL. If the input signal is lost and becomes floating for any reason, the output is pulled low. Also, with the large changes in voltage on the GND of the driver IC, it is possible for the input signals to appear negative if the GND bounces high during a switching edge. This driver addresses this concern by handling up to -5 V continuously on the input (IN) or enable (EN) during these events.

The UCC27531 comes in a 3 x 3-mm, industry-standard SOT-23 package, which is very competitive with a discrete two-transistor solution that has a discrete level shifter without negative-input capability or added protections. Beyond the obvious space savings, integrating the UCC27531's functions into a single IC package increases the system's overall reliability.

This single-channel driver is an attractive option because it can be located very close to the power-switch gate. Placement is more flexible than for a combination high-side/low-side gate driver in a single IC. This flexibility helps minimize the inductance between the driver and

power switch and gives the designer better control of the switch's gate. Figure 2 shows how many high-power switches are in just a single phase of a DC-to-AC stage. Over a complete three-phase system with multiple conversions between DC and AC and back, and with boost stages of DC-to-DC conversion also needed in some applications, there becomes a need for many gate drivers. Each one must be strategically placed on the PCB to ensure a proper design.

Conclusion

In renewable-energy applications, conversion of power generated from solar arrays and wind turbines presents unique challenges to the system designer. These challenges include high voltages and power levels, meeting safety and reliability requirements, and the overall complexity of the completely interconnected system. Although gate drivers for power switches seem like a small part of the total system control and power flow, they are actually very important to the overall design performance.

References

1. F. Blaabjerg et al., "Power electronics and reliability in renewable energy systems," presented at 21st IEEE International Symposium on Industrial Electronics, Hangzhou, China, May 28–31, 2012.
2. Veda Prakash Galigekere and Marian K. Kazimierczuk. (year, month). "Role of power electronics in renewable energy systems" [Online]. Available under "White Papers" at www.magnelab.com
3. Bob Calanan. (2011, Jan.). "Application considerations for silicon carbide MOSFETs" [Online]. Available under "Power Application Notes" at www.cree.com/power/document-library

Related Web sites

Power Management:

www.ti.com/power-aaaj

www.ti.com/ucc27531-aaaj

Subscribe to the AAJ:

www.ti.com/subscribe-aaaj

How to pick a linear regulator for noise-sensitive applications

By Sureena Gupta

Marketing Engineer

Noise-sensitive applications require a power supply that generates low internal noise and rejects noise from the power source. These applications include test and measurement applications, medical equipment, communication equipment, base stations, and many others. A low-noise power supply is used to power a signal chain that includes data converters, amplifiers, clocks, jitter cleaners, PLLs, analog front ends and many other devices. A low-noise power solution is essential to preserving signal accuracy and integrity. This article addresses criteria and parameters to consider in designing such a power solution, including important specifications for picking a linear regulator.

The terms “power supply ripple rejection” (PSRR) and “linear regulator” often are used together. The linear regulator’s high ripple rejection makes it an integral part of a power solution. PSRR is a measure of how well the regulator filters a circuit by rejecting noise or ripple coming from the power-supply input at various frequencies. In both low-dropout regulators (LDOs) and linear regulators, PSRR is a measure of output ripple compared to the input ripple over a frequency range.

Since PSRR is calculated as ripple rejection, it is expected to be a negative number. However, it is represented as a positive number in the datasheet so that a higher number denotes higher noise rejection. Mathematically, it is expressed in decibels as

$$\text{PSRR} = 20 \times \log \left(\frac{V_{\text{IN_ripple}}}{V_{\text{OUT_ripple}}} \right)$$

The PSRR of a linear regulator can be divided into three frequency-range regions. The first region extends from DC to the roll-off frequency. The ripple rejection in this region is mostly dominated by open-loop gain and the bandgap reference. The second region extends from the roll-off frequency to the unity-gain frequency. The PSRR in this region is usually higher than in the first region and is mainly dominated by the open-loop gain of the regulator. The third region’s frequency range is above that of the unity-gain frequency. The output capacitor, along with the linear regulator’s parasitics (in the $V_{\text{IN-to-}}V_{\text{OUT}}$ path), dominates this region. Therefore, the values of the selected output capacitor and its equivalent series resistance are quite important. This information can be found in any datasheet.

In addition to V_{IN} , V_{OUT} , and system load requirements, an engineer needs to know the frequency range of ripple and noise in the system or power supply in order to select linear regulators with a good PSRR in that frequency range. For example, a switcher that switches at a frequency of 2 MHz may require a linear regulator that has a high PSRR at around 2 MHz. Figure 1 shows a linear regulator’s high PSRR of about 55 dB at 2 MHz that helps to remove input noise. Also, when PSRR graphs in the regulator datasheets are evaluated, it is always good to note the dropout voltage at which the PSRR is measured. High dropout voltage leads to better PSRR but reduces the device’s efficiency.

Figure 1. Plot of linear regulator’s wide-bandwidth, high PSRR

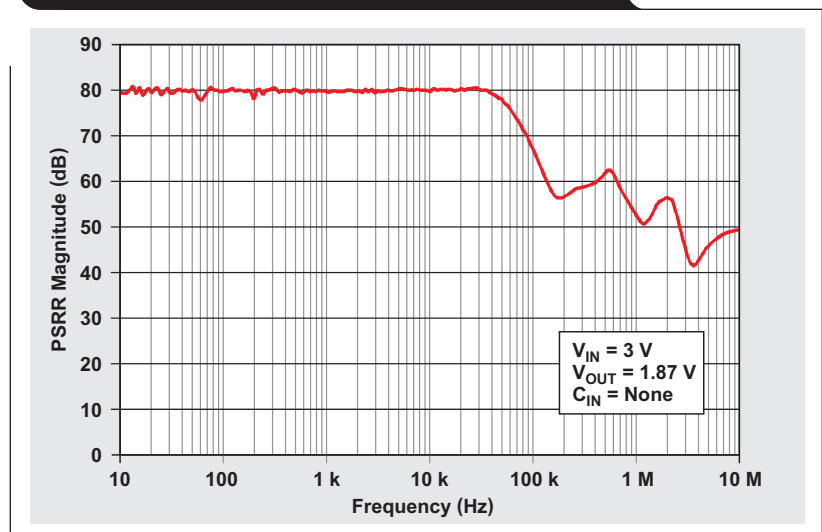


Figure 2 shows a switching regulator's spectral noise that is fed to a linear regulator. It can be seen that the switcher is operating at 500 kHz. Figure 3 shows the output spectrum of the Texas Instruments TPS7A4700 linear regulator. The spike caused by the switcher at 500 kHz has been attenuated. If the power solution is not designed for noise attenuation with high-PSRR linear regulators, the spike may show up at the output of the RF

voltage-controlled oscillators, which after mixing affect the PA performance. The spike may also fold back into the audio band and create noise in an audio application.

Usually, noise and PSRR parameters are lumped together in a linear regulator's datasheet, which causes a lot of confusion because noise and PSRR are two very different characteristics. Noise is purely a physical phenomenon that occurs with transistors and resistors

Figure 2. Typical noise spectrum from a switching regulator

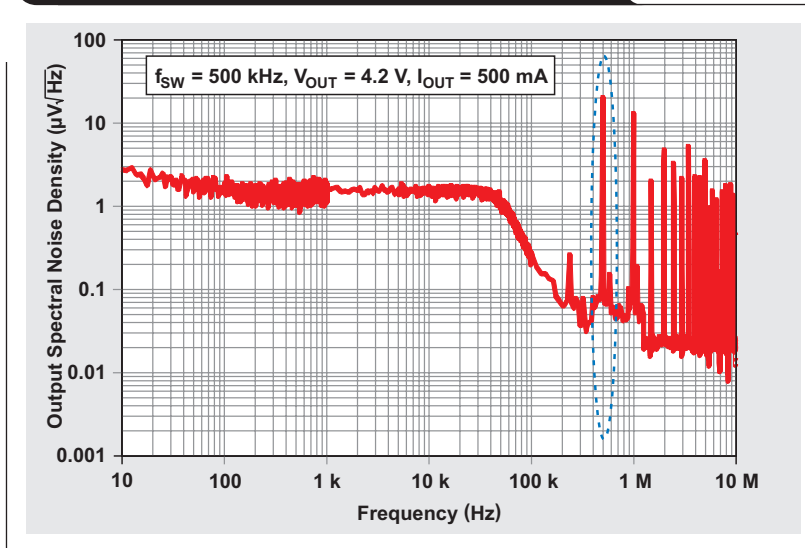
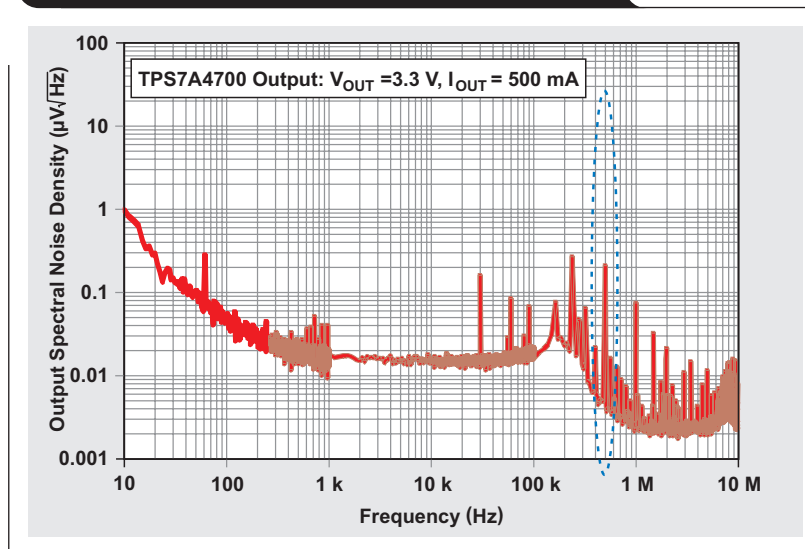


Figure 3. Output noise spectrum of TPS7A4700 linear regulator with attenuated 500-kHz spike



inside the linear regulator on a very fundamental level. This type of noise may include thermal, flicker, and shot noise. Noise is usually indicated as a curve showing spectral noise density (in $\mu\text{V}/\sqrt{\text{Hz}}$) versus frequency (Figure 4). Noise can also be indicated as integrated output noise (in μV_{RMS}), listed under the electrical characteristics table in the datasheet (Figure 5). The output noise (in μV_{RMS}) is the spectral noise density integrated over a certain frequency range and can be seen as the total noise in a specified frequency range.

The next obvious question is whether an engineer should look at spectral noise density or integrated output noise, or both. The answer depends purely on the engineer's application. For example, in RF applications where the signal does not have any dependency on the frequency, it makes more sense to look at the linear regulator's spectral noise density. However, in applications where the noise will be integrated by the system, such as powering DACs and ADCs, the engineer should look at the linear regulator's integrated output noise instead.

Conclusion

This article has discussed the important specifications that design engineers need to consider when picking a linear regulator. It has also covered the criteria and parameters to consider in designing a power solution for low-noise applications. Given these guidelines, engineers should be able to preserve signal accuracy and integrity in their applications.

Reference

1. Thomas Neu, "Power-supply design for high-speed ADCs," Analog Applications Journal (1Q 2010). Available www.ti.com/slyt366-aa

Related Web sites

Power Management:

www.ti.com/power-aa

www.ti.com/ldo-aa

www.ti.com/tps7a4700-aa

Subscribe to the AAJ:

www.ti.com/subscribe-aa

Figure 4. Spectral noise density for the TPS7A4700

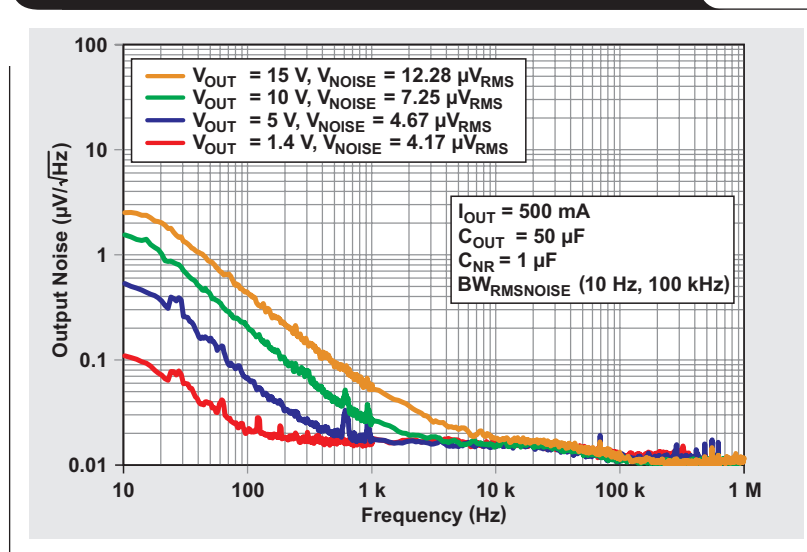


Figure 5. Excerpt from TPS7A4700 datasheet showing integrated output noise voltage

PARAMETER	TEST CONDITIONS	TYP	UNIT
V_{NOISE} Output noise voltage	$V_{\text{IN}} = 3 \text{ V}$, $V_{\text{OUT(NOM)}} = 1.4 \text{ V}$, $C_{\text{OUT}} = 50 \mu\text{F}$, $C_{\text{NR}} = 1 \mu\text{F}$, $\text{BW} = 10 \text{ Hz to } 100 \text{ kHz}$	4.17	μV_{RMS}
	$V_{\text{IN}} = 6 \text{ V}$, $V_{\text{OUT(NOM)}} = 5 \text{ V}$, $C_{\text{OUT}} = 50 \mu\text{F}$, $C_{\text{NR}} = 1 \mu\text{F}$, $\text{BW} = 10 \text{ Hz to } 100 \text{ kHz}$	4.67	μV_{RMS}

Index of Articles

Title	Issue	Page	Lit. No.
Data Converters			
Grounding in mixed-signal systems demystified, Part 1	1Q 2013	5	SLYT499
Add a digitally controlled PGA with noise filter to an ADC	1Q 2013	9	SLYT500
WEBENCH® tools and the photodetector's stability	4Q, 2012	5	SLYT487
How delta-sigma ADCs work, Part 2	4Q, 2011	5	SLYT438
How delta-sigma ADCs work, Part 1	3Q, 2011	13	SLYT423
Clock jitter analyzed in the time domain, Part 3	3Q, 2011	5	SLYT422
The IBIS model, Part 3: Using IBIS models to investigate signal-integrity issues	2Q, 2011	5	SLYT413
The IBIS model, Part 2: Determining the total quality of an IBIS model	1Q, 2011	5	SLYT400
The IBIS model: A conduit into signal-integrity analysis, Part 1	4Q, 2010	11	SLYT390
Clock jitter analyzed in the time domain, Part 2	4Q, 2010	5	SLYT389
Clock jitter analyzed in the time domain, Part 1	3Q, 2010	5	SLYT379
How digital filters affect analog audio-signal levels	2Q, 2010	5	SLYT375
How the voltage reference affects ADC performance, Part 3	4Q, 2009	5	SLYT355
How the voltage reference affects ADC performance, Part 2	3Q, 2009	13	SLYT339
Impact of sampling-clock spurs on ADC performance	3Q, 2009	5	SLYT338
How the voltage reference affects ADC performance, Part 1	2Q, 2009	5	SLYT331
Stop-band limitations of the Sallen-Key low-pass filter	4Q, 2008	5	SLYT306
A DAC for all precision occasions	3Q, 2008	5	SLYT300
Understanding the pen-interrupt (PENIRQ) operation of touch-screen controllers	2Q, 2008	5	SLYT292
Using a touch-screen controller's auxiliary inputs	4Q, 2007	5	SLYT283
Calibration in touch-screen systems	3Q, 2007	5	SLYT277
Conversion latency in delta-sigma converters	2Q, 2007	5	SLYT264
Clamp function of high-speed ADC THS1041	4Q, 2006	5	SLYT253
Using the ADS8361 with the MSP430™ USI port	3Q, 2006	5	SLYT244
Matching the noise performance of the operational amplifier to the ADC	2Q, 2006	5	SLYT237
Understanding and comparing datasheets for high-speed ADCs	1Q, 2006	5	SLYT231
Low-power, high-intercept interface to the ADS5424 14-bit, 105-MSPS converter for undersampling applications	4Q, 2005	10	SLYT223
Operating multiple oversampling data converters	4Q, 2005	5	SLYT222
Simple DSP interface for ADS784x/834x ADCs	3Q, 2005	10	SLYT210
Using resistive touch screens for human/machine interface	3Q, 2005	5	SLYT209A
Implementation of 12-bit delta-sigma DAC with MSC12xx controller	1Q, 2005	27	SLYT076
Clocking high-speed data converters	1Q, 2005	20	SLYT075
14-bit, 125-MSPS ADS5500 evaluation	1Q, 2005	13	SLYT074
Supply voltage measurement and ADC PSRR improvement in MSC12xx devices	1Q, 2005	5	SLYT073
Streamlining the mixed-signal path with the signal-chain-on-chip MSP430F169	3Q, 2004	5	SLYT078
ADS809 analog-to-digital converter with large input pulse signal	1Q, 2004	8	SLYT083
Two-channel, 500-kSPS operation of the ADS8361	1Q, 2004	5	SLYT082
Evaluation criteria for ADSL analog front end	4Q, 2003	16	SLYT091
Calculating noise figure and third-order intercept in ADCs	4Q, 2003	11	SLYT090
ADS82x ADC with non-uniform sampling clock	4Q, 2003	5	SLYT089
Interfacing op amps and analog-to-digital converters	4Q, 2002	5	SLYT104
Using direct data transfer to maximize data acquisition throughput	3Q, 2002	14	SLYT111
MSC1210 debugging strategies for high-precision smart sensors	3Q, 2002	7	SLYT110
Adjusting the A/D voltage reference to provide gain	3Q, 2002	5	SLYT109
Synchronizing non-FIFO variations of the THS1206	2Q, 2002	12	SLYT115
SHDSL AFE1230 application	2Q, 2002	5	SLYT114
Intelligent sensor system maximizes battery life: Interfacing the MSP430F123 Flash MCU, ADS7822, and TPS60311	1Q, 2002	5	SLYT123
A/D and D/A conversion of PC graphics and component video signals, Part 2: Software and control	July 2001	5	SLYT129
A/D and D/A conversion of PC graphics and component video signals, Part 1: Hardware	February 2001	11	SLYT138

Title	Issue	Page	Lit. No.
Data Converters (Continued)			
Using SPI synchronous communication with data converters — interfacing the MSP430F149 and TLV5616	February 2001	7	SLYT137
Building a simple data acquisition system using the TMS320C31 DSP	February 2001	1	SLYT136
Using quad and octal ADCs in SPI mode	November 2000	15	SLYT150
Hardware auto-identification and software auto-configuration for the TLV320AIC10 DSP Codec — a “plug-and-play” algorithm	November 2000	8	SLYT149
Smallest DSP-compatible ADC provides simplest DSP interface	November 2000	1	SLYT148
Efficiently interfacing serial data converters to high-speed DSPs	August 2000	10	SLYT160
Higher data throughput for DSP analog-to-digital converters	August 2000	5	SLYT159
New DSP development environment includes data converter plug-ins	August 2000	1	SLYT158
Introduction to phase-locked loop system modeling	May 2000	5	SLYT169
The design and performance of a precision voltage reference circuit for 14-bit and 16-bit A-to-D and D-to-A converters	May 2000	1	SLYT168
The operation of the SAR-ADC based on charge redistribution	February 2000	10	SLYT176
A methodology of interfacing serial A-to-D converters to DSPs	February 2000	1	SLYT175
Techniques for sampling high-speed graphics with lower-speed A/D converters	November 1999	5	SLYT184
Precision voltage references	November 1999	1	SLYT183
Evaluating operational amplifiers as input amplifiers for A-to-D converters	August 1999	7	SLYT193
Low-power data acquisition sub-system using the TI TLV1572	August 1999	4	SLYT192
Aspects of data acquisition system design	August 1999	1	SLYT191
Power Management			
Design of a 60-A interleaved active-clamp forward converter	1Q 2013	13	SLYT501
Power MOSFET failures in mobile PMUs: Causes and design precautions	1Q 2013	17	SLYT502
35-V, single-channel gate drivers for IGBT and MOSFET renewable-energy applications	1Q 2013	22	SLYT503
How to pick a linear regulator for noise-sensitive applications	1Q 2013	25	SLYT504
Simple open-circuit protection for boost converters in LED driver applications	4Q, 2012	21	SLYT490
LDO noise examined in detail	4Q, 2012	14	SLYT489
Harnessing wasted energy in 4- to 20-mA current-loop systems	4Q, 2012	10	SLYT488
Designing a Qi-compliant receiver coil for wireless power systems, Part 1	3Q, 2012	8	SLYT479
Easy solar-panel maximum-power-point tracking for pulsed-load applications	3Q, 2012	5	SLYT478
Design considerations for a resistive feedback divider in a DC/DC converter	2Q, 2012	18	SLYT469
Charging a three-cell nickel-based battery pack with a Li-Ion charger	2Q, 2012	14	SLYT468
Remote sensing for power supplies	2Q, 2012	12	SLYT467
A solar-powered buck/boost battery charger	2Q, 2012	8	SLYT466
Controlling switch-node ringing in synchronous buck converters	2Q, 2012	5	SLYT465
High-efficiency AC adapters for USB charging	1Q, 2012	18	SLYT451
Downslope compensation for buck converters when the duty cycle exceeds 50%	1Q, 2012	14	SLYT450
Benefits of a multiphase buck converter	1Q, 2012	8	SLYT449
Turbo-boost charger supports CPU turbo mode	1Q, 2012	5	SLYT448
Solar lantern with dimming achieves 92% efficiency	4Q, 2011	12	SLYT440
Solar charging solution provides narrow-voltage DC/DC system bus for multicell-battery applications	4Q, 2011	8	SLYT439
A boost-topology battery charger powered from a solar panel	3Q, 2011	17	SLYT424
Challenges of designing high-frequency, high-input-voltage DC/DC converters	2Q, 2011	28	SLYT415
Backlighting the tablet PC	2Q, 2011	23	SLYT414
I _Q : What it is, what it isn't, and how to use it	2Q, 2011	18	SLYT412
Benefits of a coupled-inductor SEPIC converter	2Q, 2011	14	SLYT411
Implementation of microprocessor-controlled, wide-input-voltage, SMBus smart battery charger	2Q, 2011	11	SLYT410
Fine-tuning TI's Impedance Track™ battery fuel gauge with LiFePO ₄ cells in shallow-discharge applications	1Q, 2011	13	SLYT402
An introduction to the Wireless Power Consortium standard and TI's compliant solutions	1Q, 2011	10	SLYT401
Save power with a soft Zener clamp	4Q, 2010	19	SLYT392
A low-cost, non-isolated AC/DC buck converter with no transformer	4Q, 2010	16	SLYT391
Computing power going “Platinum”	3Q, 2010	13	SLYT382
Coupled inductors broaden DC/DC converter usage	3Q, 2010	10	SLYT380

Title	Issue	Page	Lit. No.
Power Management (Continued)			
Designing DC/DC converters based on ZETA topology.....	2Q, 2010	16	SLYT372
Discrete design of a low-cost isolated 3.3- to 5-V DC/DC converter	2Q, 2010	12	SLYT371
Power-supply design for high-speed ADCs.....	1Q, 2010	12	SLYT366
Li-Ion battery-charger solutions for JEITA compliance	1Q, 2010	8	SLYT365
Fuel-gauging considerations in battery backup storage systems	1Q, 2010	5	SLYT364
Efficiency of synchronous versus nonsynchronous buck converters.....	4Q, 2009	15	SLYT358
Designing a multichemistry battery charger	4Q, 2009	13	SLYT357
Using power solutions to extend battery life in MSP430™ applications.....	4Q, 2009	10	SLYT356
Reducing radiated EMI in WLED drivers	3Q, 2009	17	SLYT340
Selecting the right charge-management solution.....	2Q, 2009	18	SLYT334
Designing a linear Li-Ion battery charger with power-path control.....	2Q, 2009	12	SLYT333
Taming linear-regulator inrush currents.....	2Q, 2009	9	SLYT332
Using a portable-power boost converter in an isolated flyback application	1Q, 2009	19	SLYT323
Cell balancing buys extra run time and battery life.....	1Q, 2009	14	SLYT322
Improving battery safety, charging, and fuel gauging in portable media applications	1Q, 2009	9	SLYT321
Paralleling power modules for high-current applications	1Q, 2009	5	SLYT320
Designing DC/DC converters based on SEPIC topology	4Q, 2008	18	SLYT309
Compensating and measuring the control loop of a high-power LED driver	4Q, 2008	14	SLYT308
Getting the most battery life from portable systems.....	4Q, 2008	8	SLYT307
New current-mode PWM controllers support boost, flyback, SEPIC, and LED-driver applications	3Q, 2008	9	SLYT302
Battery-charger front-end IC improves charging-system safety.....	2Q, 2008	14	SLYT294
Understanding output voltage limitations of DC/DC buck converters.....	2Q, 2008	11	SLYT293
Using a buck converter in an inverting buck-boost topology	4Q, 2007	16	SLYT286
Host-side gas-gauge-system design considerations for single-cell handheld applications	4Q, 2007	12	SLYT285
Driving a WLED does not always require 4 V	4Q, 2007	9	SLYT284
Simultaneous power-down sequencing with the TPS74x01 family of linear regulators.....	3Q, 2007	20	SLYT281
Get low-noise, low-ripple, high-PSRR power with the TPS717xx	3Q, 2007	17	SLYT280
TPS6108x: A boost converter with extreme versatility.....	3Q, 2007	14	SLYT279
Power-management solutions for telecom systems improve performance, cost, and size.....	3Q, 2007	10	SLYT278
Current balancing in four-pair, high-power PoE applications.....	2Q, 2007	11	SLYT270
Enhanced-safety, linear Li-Ion battery charger with thermal regulation and input overvoltage protection	2Q, 2007	8	SLYT269
Power management for processor core voltage requirements	1Q, 2007	11	SLYT261
LDO white-LED driver TPS7510x provides incredibly small solution size	1Q, 2007	9	SLYT260
Selecting the correct IC for power-supply applications.....	1Q, 2007	5	SLYT259
Fully integrated TPS6300x buck-boost converter extends Li-Ion battery life	4Q, 2006	15	SLYT256
bq25012 single-chip, Li-Ion charger and dc/dc converter for <i>Bluetooth</i> ® headsets.....	4Q, 2006	13	SLYT255
A 3-A, 1.2-V _{OUT} linear regulator with 80% efficiency and P _{LOST} < 1 W	4Q, 2006	10	SLYT254
Complete battery-pack design for one- or two-cell portable applications.....	3Q, 2006	14	SLYT248
Single-chip bq2403x power-path manager charges battery while powering system.....	3Q, 2006	12	SLYT247
TPS65552A powers portable photoflash.....	3Q, 2006	10	SLYT246
TPS61059 powers white-light LED as photoflash or movie light	3Q, 2006	8	SLYT245
Powering today's multi-rail FPGAs and DSPs, Part 2	2Q, 2006	18	SLYT240
Wide-input dc/dc modules offer maximum design flexibility	2Q, 2006	13	SLYT239
TLC5940 PWM dimming provides superior color quality in LED video displays	2Q, 2006	10	SLYT238
Practical considerations when designing a power supply with the TPS6211x	1Q, 2006	17	SLYT234
TPS79918 RF LDO supports migration to StrataFlash® Embedded Memory (P30)	1Q, 2006	14	SLYT233
Powering today's multi-rail FPGAs and DSPs, Part 1	1Q, 2006	9	SLYT232
TLC5940 dot correction compensates for variations in LED brightness.....	4Q, 2005	21	SLYT225
Li-Ion switching charger integrates power FETs.....	4Q, 2005	19	SLYT224
New power modules improve surface-mount manufacturability	3Q, 2005	18	SLYT212
Miniature solutions for voltage isolation.....	3Q, 2005	13	SLYT211
Understanding power supply ripple rejection in linear regulators.....	2Q, 2005	8	SLYT202
Understanding noise in linear regulators	2Q, 2005	5	SLYT201
A better bootstrap/bias supply circuit.....	1Q, 2005	33	SLYT077
Tips for successful power-up of today's high-performance FPGAs	3Q, 2004	11	SLYT079

Title	Issue	Page	Lit. No.
Power Management (Continued)			
LED-driver considerations	1Q, 2004	14	SLYT084
UCC28517 100-W PFC power converter with 12-V, 8-W bias supply, Part 2.	4Q, 2003	21	SLYT092
UCC28517 100-W PFC power converter with 12-V, 8-W bias supply, Part 1.	3Q, 2003	13	SLYT097
Soft-start circuits for LDO linear regulators.	3Q, 2003	10	SLYT096
Auto-Track™ voltage sequencing simplifies simultaneous power-up and power-down.	3Q, 2003	5	SLYT095
Using the TPS61042 white-light LED driver as a boost converter.	1Q, 2003	7	SLYT101
Load-sharing techniques: Paralleling power modules with overcurrent protection	1Q, 2003	5	SLYT100
Understanding piezoelectric transformers in CCFL backlight applications.	4Q, 2002	18	SLYT107
Power conservation options with dynamic voltage scaling in portable DSP designs	4Q, 2002	12	SLYT106
Using the UCC3580-1 controller for highly efficient 3.3-V/100-W isolated supply design	4Q, 2002	8	SLYT105
Powering electronics from the USB port	2Q, 2002	28	SLYT118
Optimizing the switching frequency of ADSL power supplies	2Q, 2002	23	SLYT117
SWIFT™ Designer power supply design program.	2Q, 2002	15	SLYT116
Why use a wall adapter for ac input power?	1Q, 2002	18	SLYT126
Comparing magnetic and piezoelectric transformer approaches in CCFL applications.	1Q, 2002	12	SLYT125
Power control design key to realizing InfiniBand SM benefits.	1Q, 2002	10	SLYT124
Runtime power control for DSPs using the TPS62000 buck converter	July 2001	15	SLYT131
Power supply solution for DDR bus termination	July 2001	9	SLYT130
–48-V/+48-V hot-swap applications	February 2001	20	SLYT140
Optimal design for an interleaved synchronous buck converter under high-slew-rate, load-current transient conditions	February 2001	15	SLYT139
Comparison of different power supplies for portable DSP solutions working from a single-cell battery	November 2000	24	SLYT152
Understanding the load-transient response of LDOs	November 2000	19	SLYT151
Optimal output filter design for microprocessor or DSP power supply	August 2000	22	SLYT162
Advantages of using PMOS-type low-dropout linear regulators in battery applications	August 2000	16	SLYT161
Low-cost, minimum-size solution for powering future-generation Celeron™-type processors with peak currents up to 26 A.	May 2000	14	SLYT171
Simple design of an ultra-low-ripple DC/DC boost converter with TPS60100 charge pump.	May 2000	11	SLYT170
Powering Celeron-type microprocessors using TI's TPS5210 and TPS5211 controllers	February 2000	20	SLYT178
Power supply solutions for TI DSPs using synchronous buck converters.	February 2000	12	SLYT177
Understanding the stable range of equivalent series resistance of an LDO regulator	November 1999	14	SLYT187
Synchronous buck regulator design using the TI TPS5211 high-frequency hysteretic controller	November 1999	10	SLYT186
TI TPS5602 for powering TI's DSP	November 1999	8	SLYT185
Migrating from the TI TL770x to the TI TLC770x.	August 1999	14	SLYT196
Extended output voltage adjustment (0 V to 3.5 V) using the TI TPS5210	August 1999	13	SLYT195
Stability analysis of low-dropout linear regulators with a PMOS pass element.	August 1999	10	SLYT194
Interface (Data Transmission)			
Design considerations for system-level ESD circuit protection	4Q, 2012	28	SLYT492
How to design an inexpensive HART transmitter	4Q, 2012	24	SLYT491
Data-rate independent half-duplex repeater design for RS-485.	3Q, 2012	15	SLYT480
Extending the SPI bus for long-distance communication.	4Q, 2011	16	SLYT441
Industrial data-acquisition interfaces with digital isolators.	3Q, 2011	24	SLYT426
Isolated RS-485 transceivers support DMX512 stage lighting and special-effects applications	3Q, 2011	21	SLYT425
Designing an isolated I ² C Bus [®] interface by using digital isolators	1Q, 2011	17	SLYT403
Interfacing high-voltage applications to low-power controllers	4Q, 2010	20	SLYT393
Magnetic-field immunity of digital capacitive isolators	3Q, 2010	19	SLYT381
Designing with digital isolators	2Q, 2009	21	SLYT335
Message priority inversion on a CAN bus.	1Q, 2009	25	SLYT325
RS-485: Passive failsafe for an idle bus.	1Q, 2009	22	SLYT324
Cascading of input serializers boosts channel density for digital inputs	3Q, 2008	16	SLYT301
When good grounds turn bad—isolate!.	3Q, 2008	11	SLYT298
Enabling high-speed USB OTG functionality on TI DSPs.	2Q, 2007	18	SLYT271
Detection of RS-485 signal loss	4Q, 2006	18	SLYT257
Improved CAN network security with TI's SN65HVD1050 transceiver	3Q, 2006	17	SLYT249

Title	Issue	Page	Lit. No.
Interface (Data Transmission) (Continued)			
Device spacing on RS-485 buses	2Q, 2006	25	SLYT241
Maximizing signal integrity with M-LVDS backplanes	2Q, 2005	11	SLYT203
Failsafe in RS-485 data buses	3Q, 2004	16	SLYT080
The RS-485 unit load and maximum number of bus connections	1Q, 2004	21	SLYT086
Estimating available application power for Power-over-Ethernet applications	1Q, 2004	18	SLYT085
Power consumption of LVPECL and LVDS	1Q, 2002	23	SLYT127
The SN65LVDS33/34 as an ECL-to-LVTTL converter	July 2001	19	SLYT132
The Active Fail-Safe feature of the SN65LVDS32A	November 2000	35	SLYT154
A statistical survey of common-mode noise	November 2000	30	SLYT153
Performance of LVDS with different cables	August 2000	30	SLYT163
LVDS: The ribbon cable connection	May 2000	19	SLYT172
LVDS receivers solve problems in non-LVDS applications	February 2000	33	SLYT180
Skew definition and jitter analysis	February 2000	29	SLYT179
Keep an eye on the LVDS input levels	November 1999	17	SLYT188
TIA/EIA-568A Category 5 cables in low-voltage differential signaling (LVDS)	August 1999	16	SLYT197
Amplifiers: Audio			
Precautions for connecting APA outputs to other devices	2Q, 2010	22	SLYT373
Audio power amplifier measurements, Part 2	1Q, 2002	26	SLYT128
Audio power amplifier measurements	July 2001	40	SLYT135
An audio circuit collection, Part 3	July 2001	34	SLYT134
An audio circuit collection, Part 2	February 2001	41	SLYT145
Notebook computer upgrade path for audio power amplifiers	February 2001	27	SLYT142
1.6- to 3.6-volt BTL speaker driver reference design	February 2001	23	SLYT141
An audio circuit collection, Part 1	November 2000	39	SLYT155
PCB layout for the TPA005D1x and TPA032D0x Class-D APAs	February 2000	39	SLYT182
Power supply decoupling and audio signal filtering for the Class-D audio power amplifier	August 1999	24	SLYT199
Reducing the output filter of a Class-D amplifier	August 1999	19	SLYT198
Amplifiers: Op Amps			
Using a fixed threshold in ultrasonic distance-ranging automotive applications	3Q, 2012	19	SLYT481
Source resistance and noise considerations in amplifiers	2Q, 2012	23	SLYT470
Measuring op amp settling time by using sample-and-hold technique	1Q, 2012	21	SLYT452
Converting single-ended video to differential video in single-supply systems	3Q, 2011	29	SLYT427
Using single-supply fully differential amplifiers with negative input voltages to drive ADCs	4Q, 2010	26	SLYT394
Operational amplifier gain stability, Part 3: AC gain-error analysis	3Q, 2010	23	SLYT383
Operational amplifier gain stability, Part 2: DC gain-error analysis	2Q, 2010	24	SLYT374
Interfacing op amps to high-speed DACs, Part 3: Current-sourcing DACs simplified	1Q, 2010	32	SLYT368
Signal conditioning for piezoelectric sensors	1Q, 2010	24	SLYT369
Operational amplifier gain stability, Part 1: General system analysis	1Q, 2010	20	SLYT367
Interfacing op amps to high-speed DACs, Part 2: Current-sourcing DACs	4Q, 2009	23	SLYT360
Using fully differential op amps as attenuators, Part 3: Single-ended unipolar input signals	4Q, 2009	19	SLYT359
Using the infinite-gain, MFB filter topology in fully differential active filters	3Q, 2009	33	SLYT343
Interfacing op amps to high-speed DACs, Part 1: Current-sinking DACs	3Q, 2009	24	SLYT342
Using fully differential op amps as attenuators, Part 2: Single-ended bipolar input signals	3Q, 2009	21	SLYT341
Using fully differential op amps as attenuators, Part 1: Differential bipolar input signals	2Q, 2009	33	SLYT336
Output impedance matching with fully differential operational amplifiers	1Q, 2009	29	SLYT326
A dual-polarity, bidirectional current-shunt monitor	4Q, 2008	29	SLYT311
Input impedance matching with fully differential amplifiers	4Q, 2008	24	SLYT310
A new filter topology for analog high-pass filters	3Q, 2008	18	SLYT299
New zero-drift amplifier has an I_Q of 17 μ A	2Q, 2007	22	SLYT272
Accurately measuring ADC driving-circuit settling time	1Q, 2007	14	SLYT262
Low-cost current-shunt monitor IC revives moving-coil meter design	2Q, 2006	27	SLYT242
High-speed notch filters	1Q, 2006	19	SLYT235
Getting the most out of your instrumentation amplifier design	4Q, 2005	25	SLYT226
So many amplifiers to choose from: Matching amplifiers to applications	3Q, 2005	24	SLYT213
Auto-zero amplifiers ease the design of high-precision circuits	2Q, 2005	19	SLYT204

Title	Issue	Page	Lit. No.
Amplifiers: Op Amps (Continued)			
Active filters using current-feedback amplifiers	3Q, 2004	21	SLYT081
Integrated logarithmic amplifiers for industrial applications	1Q, 2004	28	SLYT088
Op amp stability and input capacitance	1Q, 2004	24	SLYT087
Calculating noise figure in op amps	4Q, 2003	31	SLYT094
Expanding the usability of current-feedback amplifiers	3Q, 2003	23	SLYT099
Video switcher using high-speed op amps	3Q, 2003	20	SLYT098
Analyzing feedback loops containing secondary amplifiers	1Q, 2003	14	SLYT103
RF and IF amplifiers with op amps	1Q, 2003	9	SLYT102
Active output impedance for ADSL line drivers	4Q, 2002	24	SLYT108
FilterPro™ low-pass design tool	3Q, 2002	24	SLYT113
Using high-speed op amps for high-performance RF design, Part 2	3Q, 2002	21	SLYT112
Using high-speed op amps for high-performance RF design, Part 1	2Q, 2002	46	SLYT121
Worst-case design of op amp circuits	2Q, 2002	42	SLYT120
Fully differential amplifier design in high-speed data acquisition systems	2Q, 2002	35	SLYT119
Designing for low distortion with high-speed op amps	July 2001	25	SLYT133
Frequency response errors in voltage feedback op amps	February 2001	48	SLYT146
Pressure transducer-to-ADC application	February 2001	38	SLYT144
Fully differential amplifiers applications: Line termination, driving high-speed ADCs, and differential transmission lines	February 2001	32	SLYT143
Analysis of fully differential amplifiers	November 2000	48	SLYT157
Thermistor temperature transducer-to-ADC application	November 2000	44	SLYT156
Reducing PCB design costs: From schematic capture to PCB layout	August 2000	48	SLYT167
The PCB is a component of op amp design	August 2000	42	SLYT166
Fully differential amplifiers	August 2000	38	SLYT165
Design of op amp sine wave oscillators	August 2000	33	SLYT164
Using a decompensated op amp for improved performance	May 2000	26	SLYT174
Sensor to ADC — analog interface design	May 2000	22	SLYT173
Matching operational amplifier bandwidth with applications	February 2000	36	SLYT181
Reducing crosstalk of an op amp on a PCB	November 1999	23	SLYT190
Single-supply op amp design	November 1999	20	SLYT189
Low-Power RF			
Selecting antennas for low-power wireless applications	2Q, 2008	20	SLYT296
Using the CC2430 and TIMAC for low-power wireless sensor applications: A power- consumption study	2Q, 2008	17	SLYT295
General Interest			
High-definition haptics: Feel the difference!	3Q, 2012	29	SLYT483
Applying acceleration and deceleration profiles to bipolar stepper motors	3Q, 2012	24	SLYT482
Industrial flow meters/flow transmitters	2Q, 2012	29	SLYT471
Analog linearization of resistance temperature detectors	4Q, 2011	21	SLYT442
Spreadsheet modeling tool helps analyze power- and ground-plane voltage drops to keep core voltages within tolerance	2Q, 2007	29	SLYT273
Analog design tools	2Q, 2002	50	SLYT122
Synthesis and characterization of nickel manganite from different carboxylate precursors for thermistor sensors	February 2001	52	SLYT147

TI Worldwide Technical Support

Internet

TI Semiconductor Product Information Center Home Page

support.ti.com

TI E2E™ Community Home Page

e2e.ti.com

Product Information Centers

Americas	Phone	+1(512) 434-1560
Brazil	Phone	0800-891-2616
Mexico	Phone	0800-670-7544
	Fax	+1(972) 927-6377
	Internet/Email	support.ti.com/sc/pic/americas.htm

Europe, Middle East, and Africa

Phone	
European Free Call	00800-ASK-TEXAS (00800 275 83927)
International	+49 (0) 8161 80 2121
Russian Support	+7 (4) 95 98 10 701

Note: The European Free Call (Toll Free) number is not active in all countries. If you have technical difficulty calling the free call number, please use the international number above.

Fax	+ (49) (0) 8161 80 2045
Internet	www.ti.com/asktexas
Direct Email	asktexas@ti.com

Japan

Phone	Domestic	0120-92-3326
Fax	International	+81-3-3344-5317
	Domestic	0120-81-0036
Internet/Email	International	support.ti.com/sc/pic/japan.htm
	Domestic	www.tij.co.jp/pic

Asia

Phone	
International	+91-80-41381665
Domestic	<u>Toll-Free Number</u>
Note: Toll-free numbers do not support mobile and IP phones.	
Australia	1-800-999-084
China	800-820-8682
Hong Kong	800-96-5941
India	1-800-425-7888
Indonesia	001-803-8861-1006
Korea	080-551-2804
Malaysia	1-800-80-3973
New Zealand	0800-446-934
Philippines	1-800-765-7404
Singapore	800-886-1028
Taiwan	0800-006800
Thailand	001-800-886-0010
Fax	+8621-23073686
Email	tiasia@ti.com or ti-china@ti.com
Internet	support.ti.com/sc/pic/asia.htm

Important Notice: The products and services of Texas Instruments Incorporated and its subsidiaries described herein are sold subject to TI's standard terms and conditions of sale. Customers are advised to obtain the most current and complete information about TI products and services before placing orders. TI assumes no liability for applications assistance, customer's applications or product designs, software performance, or infringement of patents. The publication of information regarding any other company's products or services does not constitute TI's approval, warranty or endorsement thereof.

A090712

Auto-Track, E2E, FilterPro, Impedance Track, MSP430, OMAP, and SWIFT are trademarks and WEBENCH and DLP are registered trademarks of Texas Instruments. The *Bluetooth* word mark and logos are owned by the Bluetooth SIG, Inc., and any use of such marks by Texas Instruments is under license. Celeron is a trademark and StrataFlash is a registered trademark of Intel Corporation. I²C Bus is a registered trademark of NXP B.V. Corporation. InfiniBand is a service mark of the InfiniBand Trade Association. All other trademarks are the property of their respective owners.

IMPORTANT NOTICE

Texas Instruments Incorporated and its subsidiaries (TI) reserve the right to make corrections, enhancements, improvements and other changes to its semiconductor products and services per JESD46, latest issue, and to discontinue any product or service per JESD48, latest issue. Buyers should obtain the latest relevant information before placing orders and should verify that such information is current and complete. All semiconductor products (also referred to herein as "components") are sold subject to TI's terms and conditions of sale supplied at the time of order acknowledgment.

TI warrants performance of its components to the specifications applicable at the time of sale, in accordance with the warranty in TI's terms and conditions of sale of semiconductor products. Testing and other quality control techniques are used to the extent TI deems necessary to support this warranty. Except where mandated by applicable law, testing of all parameters of each component is not necessarily performed.

TI assumes no liability for applications assistance or the design of Buyers' products. Buyers are responsible for their products and applications using TI components. To minimize the risks associated with Buyers' products and applications, Buyers should provide adequate design and operating safeguards.

TI does not warrant or represent that any license, either express or implied, is granted under any patent right, copyright, mask work right, or other intellectual property right relating to any combination, machine, or process in which TI components or services are used. Information published by TI regarding third-party products or services does not constitute a license to use such products or services or a warranty or endorsement thereof. Use of such information may require a license from a third party under the patents or other intellectual property of the third party, or a license from TI under the patents or other intellectual property of TI.

Reproduction of significant portions of TI information in TI data books or data sheets is permissible only if reproduction is without alteration and is accompanied by all associated warranties, conditions, limitations, and notices. TI is not responsible or liable for such altered documentation. Information of third parties may be subject to additional restrictions.

Resale of TI components or services with statements different from or beyond the parameters stated by TI for that component or service voids all express and any implied warranties for the associated TI component or service and is an unfair and deceptive business practice. TI is not responsible or liable for any such statements.

Buyer acknowledges and agrees that it is solely responsible for compliance with all legal, regulatory and safety-related requirements concerning its products, and any use of TI components in its applications, notwithstanding any applications-related information or support that may be provided by TI. Buyer represents and agrees that it has all the necessary expertise to create and implement safeguards which anticipate dangerous consequences of failures, monitor failures and their consequences, lessen the likelihood of failures that might cause harm and take appropriate remedial actions. Buyer will fully indemnify TI and its representatives against any damages arising out of the use of any TI components in safety-critical applications.

In some cases, TI components may be promoted specifically to facilitate safety-related applications. With such components, TI's goal is to help enable customers to design and create their own end-product solutions that meet applicable functional safety standards and requirements. Nonetheless, such components are subject to these terms.

No TI components are authorized for use in FDA Class III (or similar life-critical medical equipment) unless authorized officers of the parties have executed a special agreement specifically governing such use.

Only those TI components which TI has specifically designated as military grade or "enhanced plastic" are designed and intended for use in military/aerospace applications or environments. Buyer acknowledges and agrees that any military or aerospace use of TI components which have **not** been so designated is solely at the Buyer's risk, and that Buyer is solely responsible for compliance with all legal and regulatory requirements in connection with such use.

TI has specifically designated certain components as meeting ISO/TS16949 requirements, mainly for automotive use. In any case of use of non-designated products, TI will not be responsible for any failure to meet ISO/TS16949.

Products

Audio	www.ti.com/audio
Amplifiers	amplifier.ti.com
Data Converters	dataconverter.ti.com
DLP® Products	www.dlp.com
DSP	dsp.ti.com
Clocks and Timers	www.ti.com/clocks
Interface	interface.ti.com
Logic	logic.ti.com
Power Mgmt	power.ti.com
Microcontrollers	microcontroller.ti.com
RFID	www.ti-rfid.com
OMAP Applications Processors	www.ti.com/omap
Wireless Connectivity	www.ti.com/wirelessconnectivity

Applications

Automotive and Transportation	www.ti.com/automotive
Communications and Telecom	www.ti.com/communications
Computers and Peripherals	www.ti.com/computers
Consumer Electronics	www.ti.com/consumer-apps
Energy and Lighting	www.ti.com/energy
Industrial	www.ti.com/industrial
Medical	www.ti.com/medical
Security	www.ti.com/security
Space, Avionics and Defense	www.ti.com/space-avionics-defense
Video and Imaging	www.ti.com/video

TI E2E Community

e2e.ti.com